

SURFACE CURRENTS INDUCED BY A PLANE WAVE ON A PARABOLIC
CYLINDER WITH A FOCAL LENGTH COMPARABLE
TO THE INCIDENT WAVELENGTH

Technical Report No. 4

F 04694-67-C-0055

Captain J. Wheatley, Contract Monitor

By

S J. Houg and R. F. Goodrich

November 1967

Prepared for

Department of the Air Force
Space and Missile Systems Organization (AFSC)
Norton Air Force Base, California 92409

This document is subject to special export controls and each transmittal to foreign governments or foreign nationals may be made only with prior approval of Space and Missile Systems Organization (SMSO), Los Angeles Air Force Station, Los Angeles, California 90045.

ABSTRACT

Expressions are obtained for surface currents excited by a plane wave on the surface of a perfectly conducting parabolic cylinder whose focal length is comparable to the incident wavelength. In the shadow region, surface currents are expressed by the residue series which represents creeping waves propagating along the surface. In the illuminated region, surface currents may be represented by the summation of a geometrical optic term and a residue series which may be defined as the reflected creeping waves. In the penumbra region, surface currents may be obtained by the series expansion of the integral representation about a point on the shadow boundary.

THE UNIVERSITY OF MICHIGAN

8525-4-T

FOREWORD

This report(SAMSO-TR-68-35) was prepared by the Radiation Laboratory of the Department of Electrical Engineering, The University of Michigan. The work was performed under Contract F 04694-67-C-0055, "Investigation of Re-entry Vehicle Surface Fields (Backscatter) (SURF)". Dr. Raymond F. Goodrich is the Principal Investigator and Mr. Burton A. Harrison, Contract Manager. The work was administered under the direction of the Air Force Space and Missile Systems Organization (AFSC), Norton Air Force Base, California, 92409 by Captain James Wheatley and was monitored by H. J. Katzman of the Aerospace Corporation.

This document is subject to special export controls and each transmittal to foreign governments or foreign nationals may be made only with prior approval of Space and Missile Systems Organization (SMSD), Los Angeles Air Force Station, Los Angeles, California 90045.

Information in this report is embargoed under the Department of State International Traffic in Arms Regulations. Private individuals or firms require a Department of State export license.

The publication of this report does not constitute Air Force Approval of the report's findings or conclusions. It is published for the exchange and stimulation of ideas.

SAMSO Approving Authority.

WILLIAM J. SCHLERF
CONTRACTING OFFICER

TABLE OF CONTENTS

	Page
ABSTRACT	iii
FOREWORD	iv
LIST OF ILLUSTRATIONS	vi
I INTRODUCTION	1
II INTEGRAL REPRESENTATION FOR SURFACE CURRENTS	3
III SURFACE CURRENTS IN THE SHADOW REGION	7
3.1 Formulation	7
3.2 Zeros of $W_n(z_0)$	11
3.3 Zeros of $'W_n(z_0)$	16
3.4 The Value of the Functions $\frac{\partial}{\partial n} W_n(z_0)$ and $\frac{\partial}{\partial n} 'W_n(z_0)$ Evaluated at Zeros	18
3.5 Creeping Waves	22
IV SURFACE CURRENTS IN THE ILLUMINATED REGION	33
4.1 Formulation	33
4.2 The Method of Geometrical Optics	36
4.3 Reflected Creeping Waves	37
V THE SURFACE CURRENT IN THE REGION OF PENUMBRA	40
REFERENCES	42
DD 1473	
DISTRIBUTION LIST	

LIST OF ILLUSTRATIONS

Figure		Page
1-1	Geometrical Optics and Creeping Waves .	2
2-1	Geometrical Optics .	4
2-2	Paths of Integration for the Function $U_n(z)$ and $W_n(z)$.	6
2-3	Paths of Integration in the Complex n-Plane .	6
3-1	Line of Zeros for the Function $W_n(z)$ When $z = \sqrt{-i} \rho$.	9
3-2	The w-Plane When $z = \sqrt{-i} \rho$; $\rho = \sqrt{2kh}$.	9
3-3	Graphical Solution for Zeros of $W_n(z)$ When $z = \sqrt{-i} \rho$.	14
3-4	Locus of Zeros of $W_n(z)$ in the m-Plane When $z = \sqrt{-i} \rho$.	15
3-5	Graphical Solution for Zeros of $'W_n(z)$ When $z = \sqrt{-i} \rho$.	19
3-6	Locus' of Zeros of $'W_n(z)$ in the m-Plane When $z = \sqrt{-i} \rho$.	20
3-7	The Surface Current Density at the Crest , $\xi = 0$.	27
3-8	$\alpha(\xi)$ Versus $\sqrt{k} \xi$.	28
3-9	$\alpha'(\xi)$ Versus $\sqrt{k} \xi$.	29
3-10	Attenuation Factor Versus Arc Length .	30
3-11	Attenuation Versus Arc Length .	31
3-12	Attenuation Factors on Parabolic Cylinders .	32
4-1	Region in the Complex m-Plane Corresponding to Asymptotic Expressions When $z = \sqrt{ik} \xi$.	35
4-2	$\ln C(m) $ versus ρ .	41

I

INTRODUCTION

The first theoretical work on the diffraction of plane electromagnetic waves by a parabolic cylinder was done by P.S. Epstein (1914). His work makes use of a series of parabolic cylinder functions. When the radius of curvature at the vertex of the cylinder is large compared to the wavelength of the incident wave many terms are required for computation.

V. Fock (1946) used an entirely different approach. He sketches the derivation of an integral for the current density on a large paraboloid of revolution. His result gives the change in current density on a large and perfect conducting parabolic cylinder as we go from the illuminated region into the shadow.

In 1954 S. O. Rice by starting with Epstein's series investigated the diffraction of plane electromagnetic waves by a parabolic cylinder. The series is converted into an integral and then the path of integration is deformed. He studied the behavior of parabolic cylinder functions of complex order in great detail.

V. I. Ivanov (1960, 1963) by following Rice's procedure derives asymptotic formulae for a field which are uniformly true for regions of the umbra and penumbra behind a large parabolic cylinder and are connected with the formulae of geometrical optics in the illuminated region. In the shadow region he interpretes the results in terms of the "geometric theory of diffraction" [Keller, 1956].

In the past work, no one has considered the solution for the small parabolic cylinder which we mean a short focal length comparable to the incident wavelength. Therefore in this report we derive the asymptotic currents excited by a plane wave on the surface of a perfect conducting small parabolic cylinder by using the residue series representation. The graphical method is applied to obtaine the location of the pole and Rice's results are used in all asymptotic expressions. Our results are sketched graphically in Fig. 1-1.

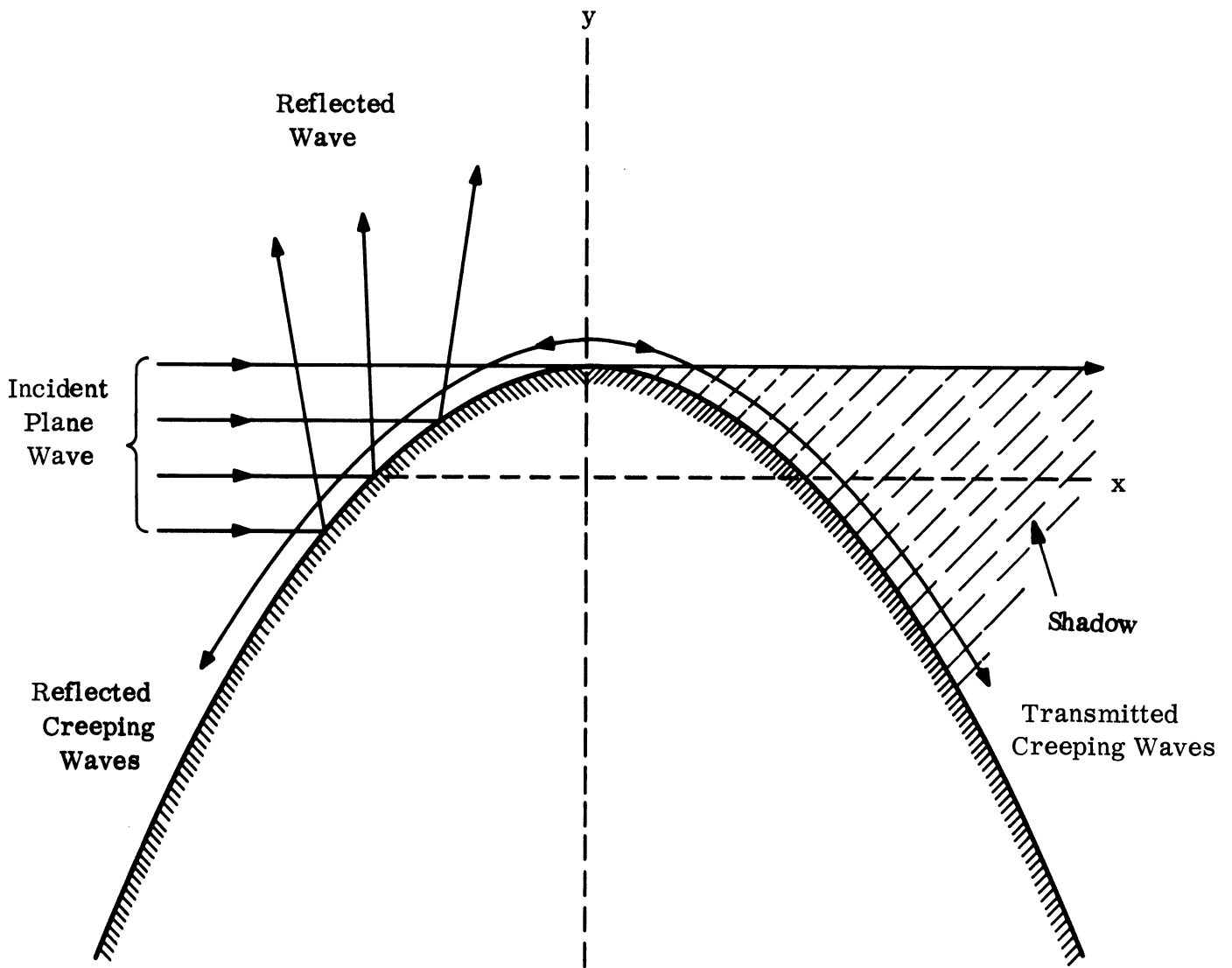


FIG. 1-1: GEOMETRICAL OPTICS AND CREEPING WAVES.

II

INTEGRAL REPRESENTATION FOR SURFACE CURRENTS

Let us consider a perfectly conducting parabolic cylinder $x^2 = 4h(h-y)$ with the focal length h and the focus at the origin of coordinates. In parabolic coordinates, $x = \xi\eta$ and $y = \frac{1}{2}(\eta^2 - \xi^2)$, the given parabolic cylinder is a coordinate surface $\eta = \sqrt{2h} \geq 0$. When $\eta = 0$ the cylinder reduces to the half-plane $x = 0$, $y \leq 0$. Let there be a plane wave $U_0 = e^{-ik(x \sin \psi - y \cos \psi)}$ with the time factor $e^{i\omega t}$ impinged upon a parabolic cylinder at an angle ψ as shown in Fig. 2-1. From Rice's (1954) results, surface currents are obtained in the form of a series

$$J_D = \sqrt{\frac{ik}{2\pi r}} e^{-ikr} \sec \frac{\psi}{2} \sum_{n=0}^{\infty} \left(-i \tan \frac{\psi}{2}\right)^n \frac{U_n(z')}{W_n(z_0)} \quad (2.1)$$

$$J_N = i \frac{1}{\sqrt{\pi}} e^{ikr} \sec \frac{\psi}{2} \sum_{n=0}^{\infty} \left(-i \tan \frac{\psi}{2}\right)^n \frac{U_n(z')}{W_n(z_0)} \quad (2.2)$$

where

$$z' = \sqrt{ik} \xi, \quad z_0 = \sqrt{-ik} \eta_0 = \sqrt{-i2kh} = \sqrt{-i} \rho.$$

J_D and J_N indicate surface currents for Dirichlet and Neumann Problem respectively. The functions $U_n(z)$ and $W_n(z)$ are defined by contour integrals of the form

$$W_n(z) = \frac{1}{2\pi i} \int_W \exp [f(t)] dt \quad (2.3)$$

$$U_n(z) = \frac{1}{2\pi i} \int_U \exp [f(t)] dt \quad (2.4)$$

THE UNIVERSITY OF MICHIGAN

8525-4-T

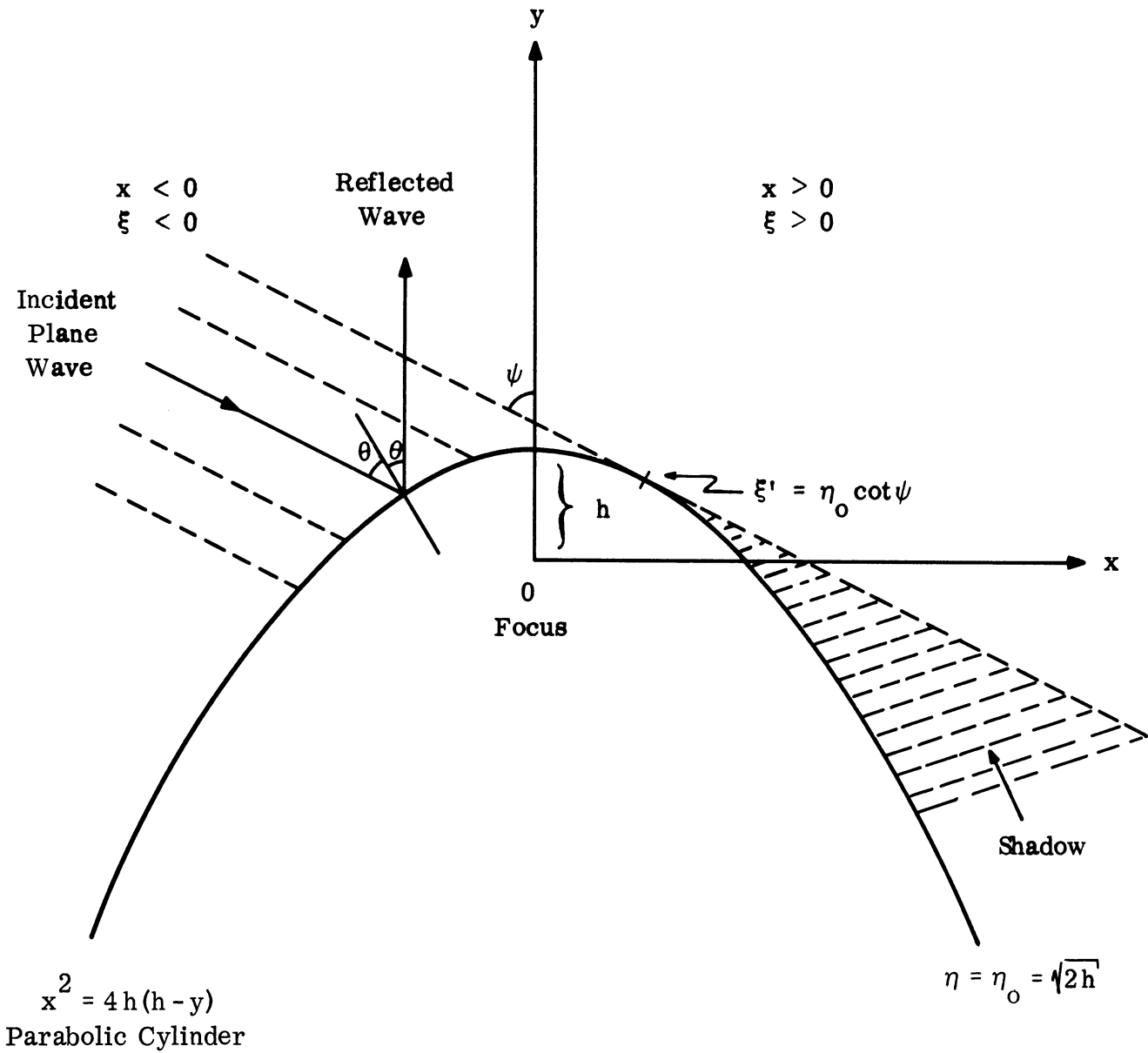


FIG. 2-1: GEOMETRICAL OPTICS

where

$$f(t) = -t^2 + 2zt - (n+1) \ln t \quad . \quad (2.5)$$

The paths of integration for $W_n(z)$ and $U_n(z)$ are indicated by W and U respectively in Fig. 2-2. The function $'W_n(z)$ is defined by

$$'W_n(z) = -z W_n(z) + \frac{\partial}{\partial z} W_n(z) \quad (2.6)$$

By Watson's transformation, the series can be converted into contour integrals with n as the complex variable of integration. Thus expressions (2.1) and (2.2) are transformed respectively into

$$J_D = \sqrt{\frac{k}{2\pi r i}} \frac{e^{-ikr}}{2} \sec \frac{\psi}{2} \int_{C_1} \frac{(i \tan \frac{\psi}{2})^n}{\sin \pi n} \frac{U_n(z')}{W_n(z_o)} dn \quad (2.7)$$

and

$$J_N = \frac{1}{\sqrt{\pi}} \frac{e^{-ikr}}{2} \sec \frac{\psi}{2} \int_{C_1} \frac{(i \tan \frac{\psi}{2})^n}{\sin \pi n} \frac{U_n(z')}{'W_n(z_o)} dn \quad (2.8)$$

with the path of integration C_1 shown in Fig. 2-3.

THE UNIVERSITY OF MICHIGAN

8525-4-T

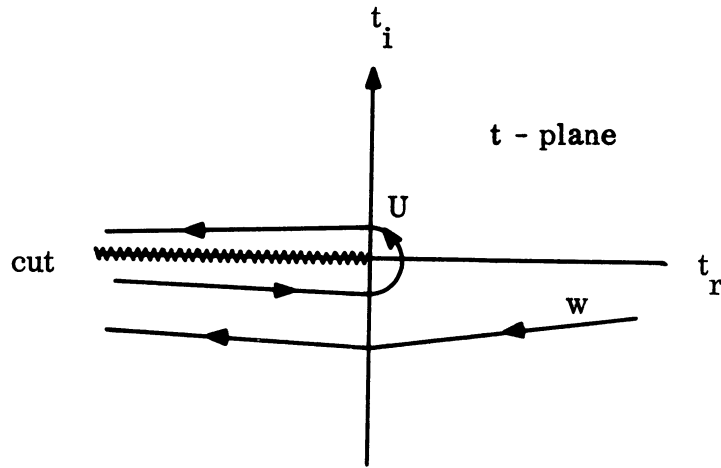


FIG. 2-2: PATHS OF INTEGRATION FOR THE FUNCTION $U_n(z)$ AND $W_n(z)$.

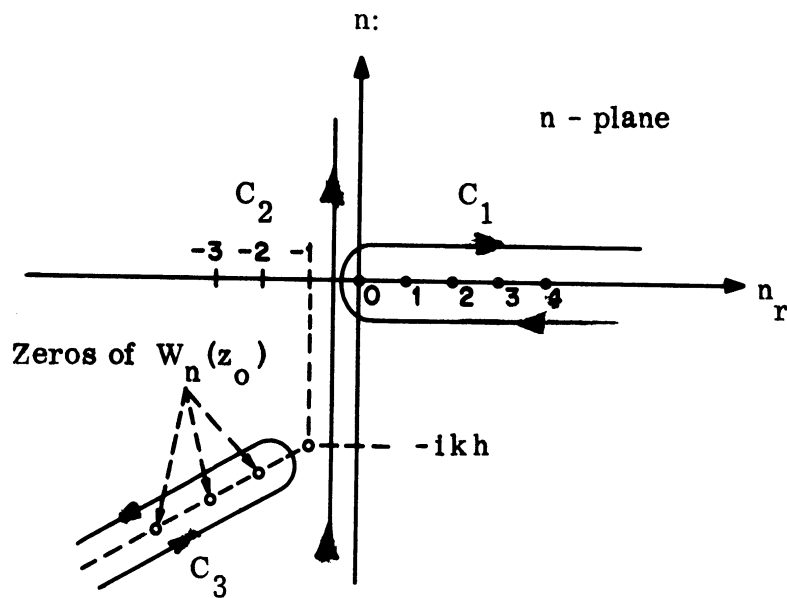


FIG. 2-3: PATHS OF INTEGRATION IN THE COMPLEX n -PLANE.

III

SURFACE CURRENTS IN THE SHADOW REGION

3.1 Formulation

It has been shown that all zeros of both function $W_n(z_o)$ and $'W_n(z_o)$ are located in the third quadrant of the n -plane, while the points $n = -1, -2, -3, \dots$ are not singular [Rice, 1954]. Therefore the contour C_1 may be deformed into C_3 contained all zeros, and the asymptote of the integral is defined by the poles of the integrand, i. e. surface currents may be expressed by the sum of the residues at the poles

$$J_D = \sqrt{\frac{ik\pi}{2r}} e^{-ikr} \sec \frac{\psi}{2} \sum_{s=1}^{\infty} \left[\frac{(i \tan \frac{\psi}{2})^n U_n(z')}{\sin \pi n \frac{\partial}{\partial n} W_n(z_o)} \right]_{n=n_s} \quad (3.1)$$

$$J_N = i \sqrt{\pi} e^{-ikr} \sec \frac{\psi}{2} \sum_{s=0}^{\infty} \left[\frac{(i \tan \frac{\psi}{2})^n U_n(z')}{\sin \pi n \frac{\partial}{\partial n} 'W_n(z_o)} \right]_{n=n'_s} \quad (3.2)$$

where n_s and n'_s are zeros of functions $W_n(z_o)$ and $'W_n(z_o)$ respectively.

In order to locate zeros, the saddle-point method of approximate integration is used to obtain asymptotic expressions for the function $W_n(z_o)$. Two saddle points in complex t -plane are obtained from (2.5) by setting $f'(t) = 0$, i. e.

$$t_o = \frac{1}{2} \left[z_o + \sqrt{z_o^2 - 2m} \right] \quad (3.3)$$

$$t_1 = \frac{1}{2} \left[z_o - \sqrt{z_o^2 - 2m} \right] \quad (3.4)$$

where $m = n + 1$.

The path of steepest descent which passes through t_0 is that branch of the curve

$$\text{Im} [f(t) - f(t_0)] = 0 \quad \text{and} \quad \text{Re} [f(t) - f(t_0)] \leq 0$$

for which t_0 is the highest point.

The path of steepest descent has been shown by Rice (1954) to have the following properties:

1) If z_0 is regarded as fixed and t_0, t_1 are functions of m defined by (3.3) and (3.4) the equation

$$\text{Im} [f(t_0) - f(t_1)] = 0 \tag{3.5}$$

defines a critical boundary in the complex m -plane. On this boundary the steepest descent contour passes through two saddle points, t_0 and t_1 , in the complex t -plane. In this case both saddle points will contribute to the asymptotic expression of the function $W_n(z_0)$. In general this critical boundary defines a region in the complex m -plane within which a function is approximately evaluated from two saddle points (Fig. 3-1).

2) If m is such that the path of integration W must be deformed along the steepest descent contour to pass two saddle points, each one will contribute to the value of $W_n(z_0)$. Furthermore, if m is such that

$$\text{Re} [f(t_0) - f(t_1)] = 0 \tag{3.6}$$

t_0 and t_1 have the same height and the two contributions have a chance of cancelling each other and giving a value of zero for $W_n(z_0)$. Thus (3.6) defines the line in the complex m -plane along which zeros of $W_n(z_0)$ are asymptotically distributed (Fig. 3-1).

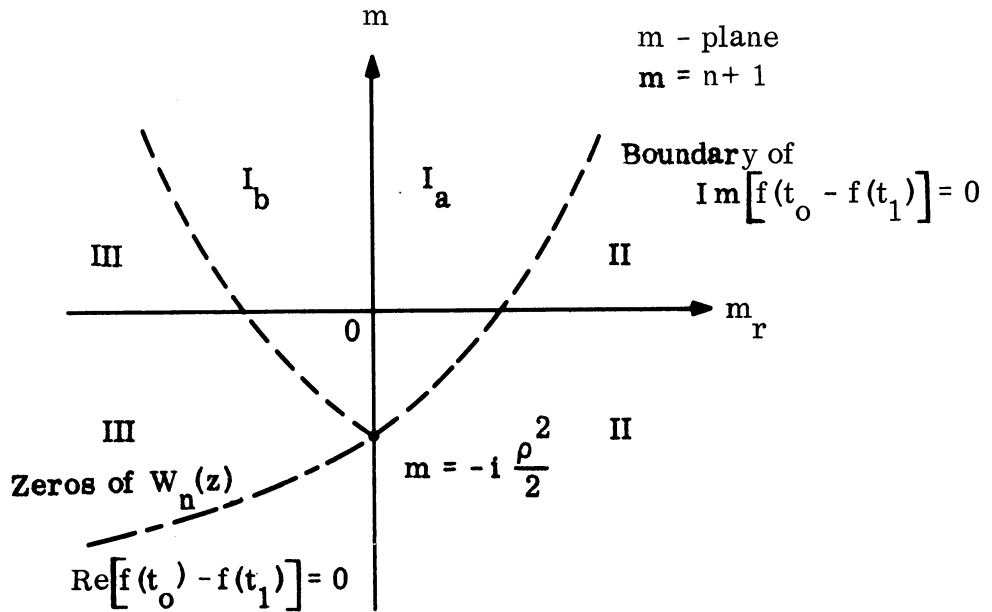


FIG. 3-1: LINE OF ZEROS FOR THE FUNCTION $W_n(z)$ WHEN $z = \sqrt{-i} \rho$.

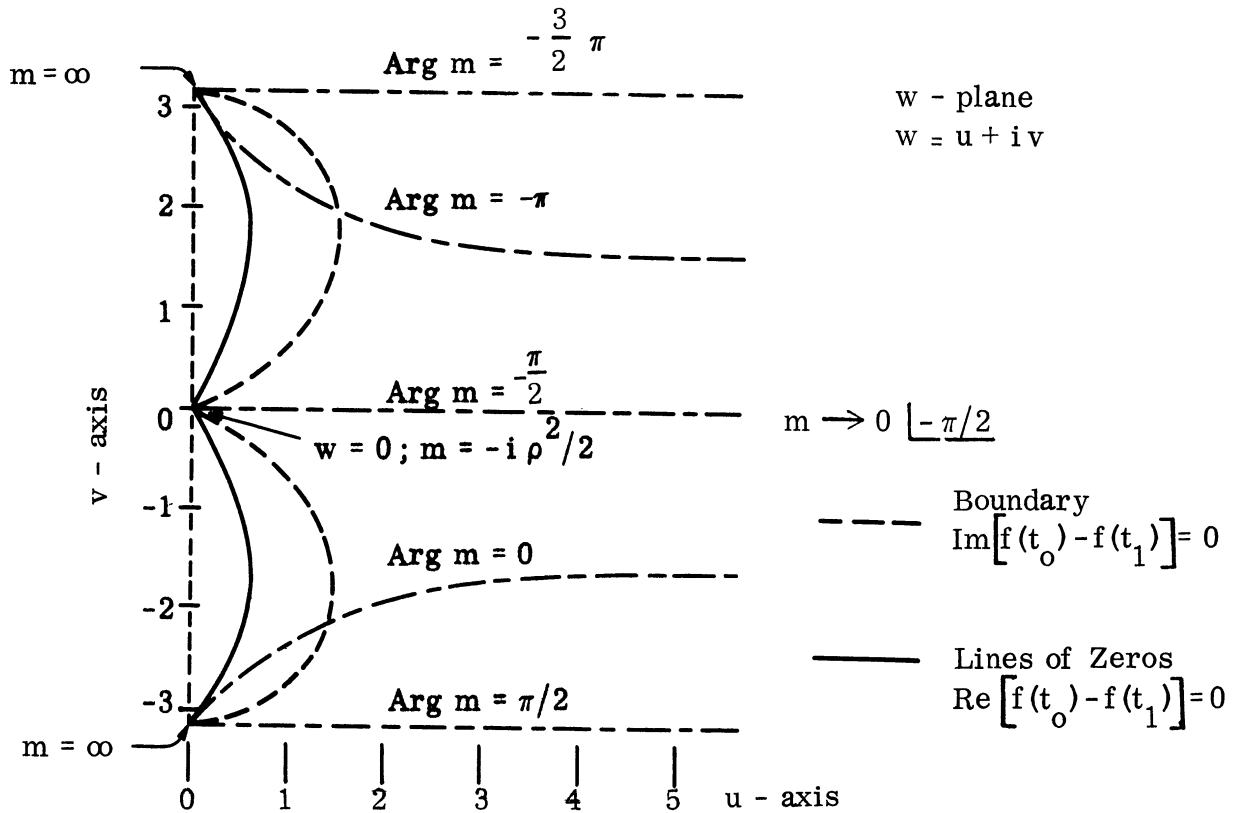


FIG. 3-2: THE w -PLANE WHEN $z = \sqrt{-i} \rho$; $\rho = \sqrt{2kh}$.

3) The lines in the complex m -plane defined by (3.5) and (3.6) may be obtained by the following transformation

$$W = \ln \left(\frac{t_0}{t_1} \right) = u + iv \quad (3.7)$$

From this transformation we obtain

$$m = n + 1 = \frac{z_0^2}{\cosh w + 1} \quad (3.8)$$

$$\begin{aligned} f(t_0) - f(t_1) &= m(\sinh w - w) \\ &= \frac{z_0^2 (\sinh w - w)}{\cosh w + 1} \end{aligned} \quad (3.9)$$

Since $|t_0| \geq |t_1|$ and $|\arg t_0 - \arg t_1| \leq \pi$ we have $u \geq 0$ and $v \leq \pi$ for mapping (Fig. 3-2).

4) For the special case $z_0 = \sqrt{-2ikh} = \sqrt{-i} \rho$, (3.9) gives

$$(\cosh u + \cos v - v \sin v) \sinh u = (\cosh u \cos v + 1) u \quad (3.10)$$

$$(\cos v + \cosh u + u \sinh u) \sin v = (\cosh u \cos v + 1) v \quad (3.11)$$

respectively for

$$\operatorname{Im} [f(t_0) - f(t_1)] = 0$$

and

$$\operatorname{Re} [f(t_0) - f(t_1)] = 0$$

(Fig. 3-2).

3.2 Zeros of $W_n(z_0)$

The zeros of $W_n(z_0)$, regarded as function n , occur when the contribution from two saddle points cancel each other. From Rice's (1954) results, the asymptotic expression of $W_n(z_0)$ for the region III (Fig. 3-1) where the path of integration passes through two saddle points t_0 and t_1 is

$$W_n(z_0) = A_0 - A_1 \tag{3.12}$$

where

$$A_0 = \frac{\sqrt{t_0} e^{f(t_0)}}{-2i \sqrt{\pi} (-i\rho^2 - 2m)^{1/4}} \tag{3.13}$$

$$A_1 = \frac{\sqrt{t_1} e^{f(t_1)}}{2 \sqrt{\pi} (-i\rho^2 - 2m)^{1/4}} \tag{3.14}$$

$$f(t_0) = \frac{m}{2} \left(1 - \ln \frac{m}{2} - \ln \frac{t_0}{t_1} \right) + \sqrt{-i} \rho t_0 \tag{3.15}$$

$$f(t_1) = \frac{m}{2} \left(1 - \ln \frac{m}{2} - \ln \frac{t_1}{t_0} \right) + \sqrt{-i} \rho t_1 \tag{3.16}$$

and

$$-\frac{3\pi}{2} \leq \arg m < \frac{\pi}{2}$$

$$-\frac{3\pi}{2} \leq \arg (-i\rho^2 - 2m) < \frac{\pi}{2}$$

$$-\frac{3\pi}{4} \leq \arg t_0 < \frac{\pi}{4}$$

$$-\frac{5\pi}{4} \leq \arg t_1 < \frac{3\pi}{4} .$$

Therefore zeros of $W_n(z_o)$ are located at

$$A_o - A_1 = 0$$

i. e.

$$\exp [f(t_o) - f(t_1)] = \frac{1}{i \sqrt{t_o/t_1}} \quad (3.17)$$

Using the transformation (3.7) and (3.9), we obtain

$$-i \rho^2 \frac{\sinh w - w}{\cosh w + 1} = - \left[\frac{w}{2} + i \frac{\pi}{2} (1 - 4s) \right] \quad (3.18)$$

where

$$s = 1, 2, 3, \dots$$

By separating the real part and the imaginary part of (3.18), we obtain two simultaneous equations

$$\begin{aligned} \rho^2 \left[(\cos v + \cosh u + u \sinh u) \sin v - (\cosh u \cos v + 1) v \right] &= \\ &= - \frac{1}{2} u \left[(\cosh u \cos v + 1)^2 + (\sinh u \sin v)^2 \right] \end{aligned} \quad (3.19)$$

$$\begin{aligned} \rho^2 \left[(\cos v + \cosh u - v \sin v) \sinh u - (\cosh u \cos v + 1) u \right] &= \\ &= \frac{1}{2} \left[v + (1 - 4s) \pi \right] \left[(\cosh u \cos v + 1)^2 + (\sinh u \sin v)^2 \right]. \end{aligned} \quad (3.20)$$

Let (3.19) be divided by (3.20), we obtain

$$\frac{(\cos v + \cosh u + u \sinh u) \sin v - (\cosh u \cos v + 1) v}{(\cos v + \cosh u - v \sin v) \sinh u - (\cosh u \cos v + 1) u} = \frac{-u}{v - (1 - 4s) \pi} \quad (3.21)$$

This equation is independent of the parameter ρ . Setting $s = 1$, we calculate the first zero as the following by graphical means.

Equation (3.21) may be approximated by a circle in the w -plane as

$$\left[u - (r - a) \right]^2 + \left[v - \frac{\pi}{2} \right]^2 = r^2 \quad (3.22)$$

where

$$r = \frac{a^2 + (\pi/2)^2}{2a}$$

$$a = u \Big|_{v = \pi/2} = 0.575, \quad s = 1$$

$$0 < u \leq a < 1 \quad .$$

For $u < 1$, (3.20) can be evaluated approximately by

$$-\rho^2 uv \sin v = \frac{1}{2} (v - 3\pi) \left[(\cos v + 1)^2 + (u \sin v)^2 \right] \quad (3.23)$$

If we plot (3.22) and (3.23) on the w -plane, the points of intersection between the two curves determine the zeros of $W_n(z_0)$. A typical plot is given in Fig. 3-3.

Mapping the zeros of $W_n(z_0)$ from the auxilliary w -plane with the help of

$$m = -i\rho^2 / (\cosh w + 1)$$

gives the location of zeros on the m -plane. If we consider ρ as the variable parameter, the locus of the first zero in the m -plane is expressed approximately by

$$m_p = -\frac{1}{2} \left[(\rho + 2.8) + i(\rho^2 + \rho + 1.4) \right] \quad (3.24)$$

where we limit the range of ρ as $0 < \rho < 10$. $\text{Re } m_p$ and $\text{Im } m_p$ are plotted in Fig. 3-4. Similarly, loci for $s = 2, 3, 4, \dots$ may be obtained by the graphical method.

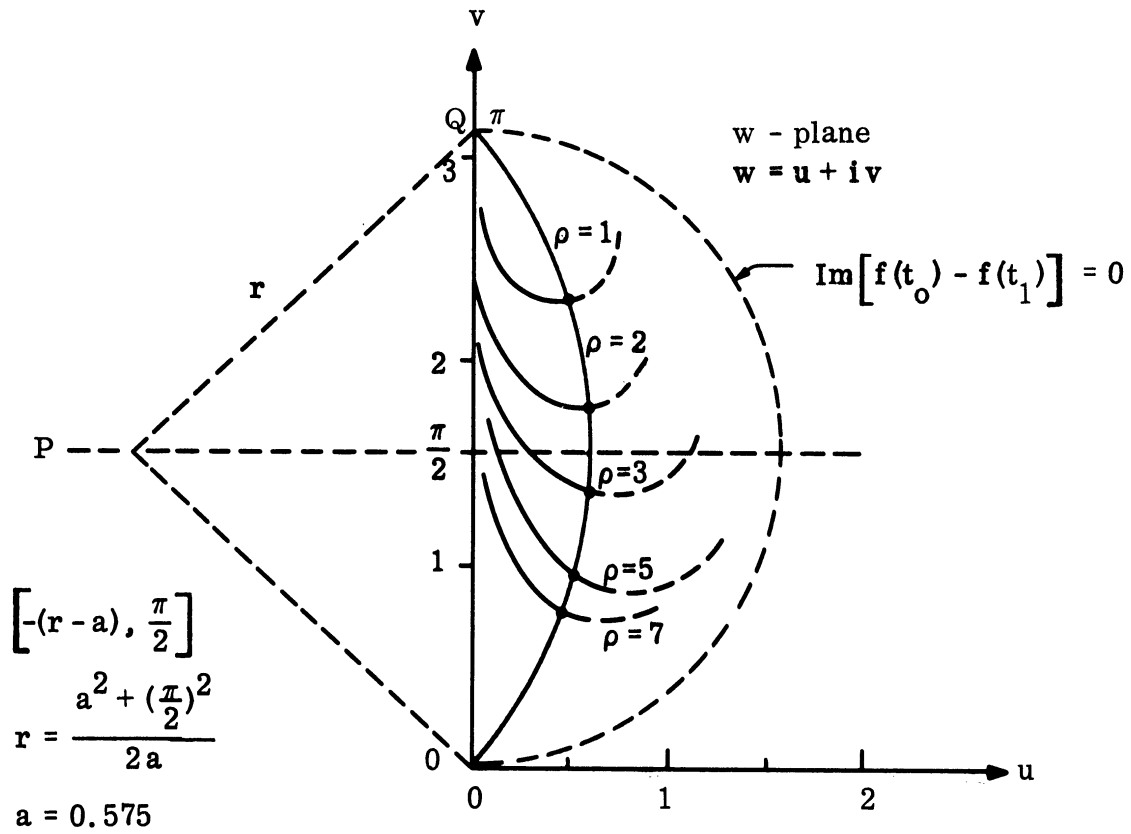


FIG. 3-3: GRAPHICAL SOLUTION FOR ZEROS OF $W_n(z)$ WHEN $z = \sqrt{-i}\rho$.

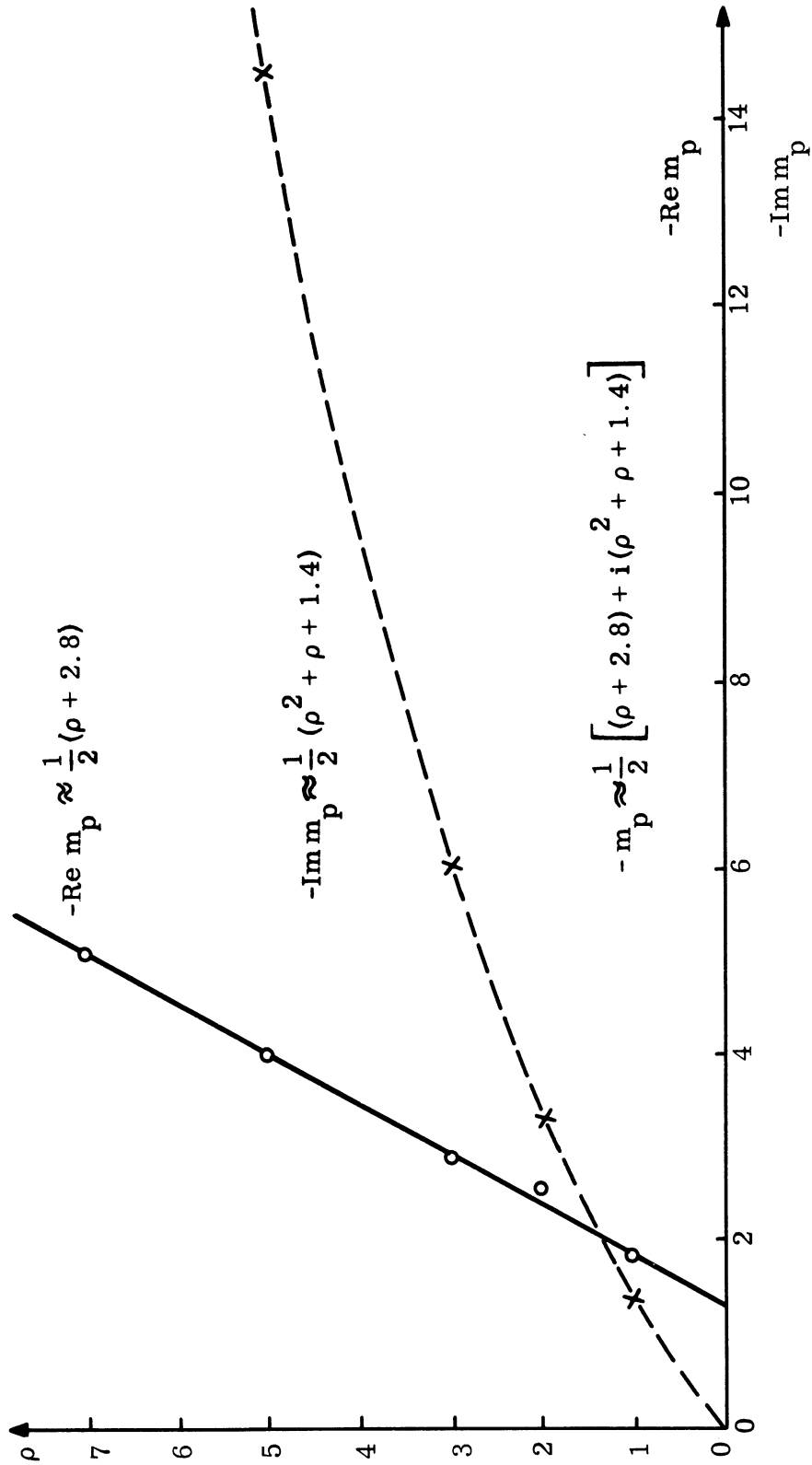


FIG. 3-4: LOCUS OF ZEROS OF $W_n(z)$ IN THE m -PLANE WHEN $z = \sqrt{-i\rho}$.

3.3 Zeros of $'W_n(z_o)$

In Neumann's problem we define the function

$$'W_n(z_o) = -z_o W_n(z_o) + \frac{\partial}{\partial z_o} W_n(z_o) \quad (3.25)$$

Here

$$W'_n(z_o) = \frac{\partial}{\partial z_o} W_n(z_o)$$

has the asymptotic expression

$$\begin{aligned} W'_n(z_o) \approx & 2t_o \left[\text{contribution of } t_o \text{ to } W_n(z_o) \right] + \\ & + 2t_1 \left[\text{contribution of } t_1 \text{ to } W_n(z_o) \right] \end{aligned} \quad (3.26)$$

from the saddle points t_o and t_1 . If the path of integration does not pass through a particular saddle point, its contribution to (3.26) is zero. Upon replacing t_o and t_1 by their expressions and subtracting the corresponding expression for $z_o W_n(z_o)$ we obtain

$$\begin{aligned} 'W_n(z_o) \approx & \sqrt{(z_o)^2 - 2m} \left[\left(t_o \text{ contribution to } W_n(z_o) \right) - \right. \\ & \left. - \left(t_1 \text{ contribution to } W_n(z_o) \right) \right]. \end{aligned} \quad (3.27)$$

When $z_o = \sqrt{-2ikh} = \sqrt{-i}\rho$, the asymptotic expression of $'W_n(z_o)$ for the case that the path of integration passes through two saddle points t_o and t_1 is

$$'W_n(z_o) = \sqrt{-i\rho^2 - 2m} [A_o + A_1] \quad (3.28)$$

where A_o and A_1 are expressed by (3.13) and (3.14) respectively.

Therefore, the zeros of $W_n(z)$ are located at

$$A_0 + A_1 = 0$$

or

$$\exp \left[f(t_0) - f(t_1) \right] = \frac{i}{\sqrt{t_0/t_1}} \quad (3.29)$$

Using the transformation $w = \ln(t_0/t_1) = u + iv$, we obtain

$$-i\rho^2 \frac{\sinh w - w}{\cosh w + 1} = i \frac{\pi}{2} (1 + 4s) - \frac{w}{2} \quad (3.30)$$

where $s = 0, 1, 2, 3, \dots$

By separating the real part and the imaginary part of (3.30) we obtain two simultaneous equations

$$\begin{aligned} \rho^2 \left[(\cos v + \cosh u + u \sinh u) \sin v - (\cosh u \cos v + 1) v \right] \\ = -\frac{1}{2} u \left[(\cosh u \cos v + 1)^2 + (\sinh u \sin v)^2 \right] \end{aligned} \quad (3.31)$$

$$\begin{aligned} \rho^2 \left[(\cos v + \cosh u - v \sin v) \sinh u - (\cosh u \cos v + 1) u \right] \\ = \frac{1}{2} \left[v - \pi (1 + 4s) \right] \left[(\cosh u \cos v + 1)^2 + (\sinh u \sin v)^2 \right]. \end{aligned} \quad (3.32)$$

Dividing (3.31) by (3.32) we have

$$\frac{(\cos v + \cosh u + \sinh u) \sin v - (\cosh u \cos v + 1) v}{(\cos v + \cosh u - v \sin v) \sinh u - (\cosh u \cos v + 1) u} = \frac{-u}{v - \pi(1+4s)} \quad (3.33)$$

Setting $s = 0$, (3.33) may be approximated by a circle in the w -plane

$$\left[u - (r - a) \right]^2 + \left[v - \frac{\pi}{2} \right]^2 = r^2 \quad (3.34)$$

where

$$r = \frac{a^2 + \left(\frac{\pi}{2}\right)^2}{2a}$$

$$a = u \Big|_{v = \pi/2} = 0.48$$

$$0 < u \leq a < 1 .$$

For $u < 1$, (3.32) may be approximated by

$$-2uv \sin v = \frac{1}{2} (v - \pi) \left[(\cos v + 1)^2 + (u \sin v)^2 \right] . \quad (3.35)$$

The location of zeros are determined by the graphical method from (3.34) and (3.35). A typical plot is shown in Fig. 3-5. Mapping the zeros from the w -plane to m -plane gives approximately the locus of the first zero as

$$m'_p = - \left(\frac{1}{\pi} \rho + \frac{1}{10} \right) - i \frac{1}{2} \rho (\rho + 1) \quad (3.36)$$

where ρ is limited in the range $0 < \rho < 10$. $\text{Re } m'_p$ and $\text{Im } m'_p$ are plotted in Fig. 3-6. Similarly, loci for $s = 1, 2, 3, \dots$ may be obtained by the graphical method.

3.4 The Value of the Functions $\frac{\partial}{\partial n} W_n(z_o)$ and $\frac{\partial}{\partial n} 'W_n(z_o)$ Evaluated at Zeros

The function $W_n(z_o)$ is defined by

$$W_n(z_o) = \frac{1}{2\pi i} \int_W e^{f(t)} dt \quad (3.37)$$

THE UNIVERSITY OF MICHIGAN

8525-4-T

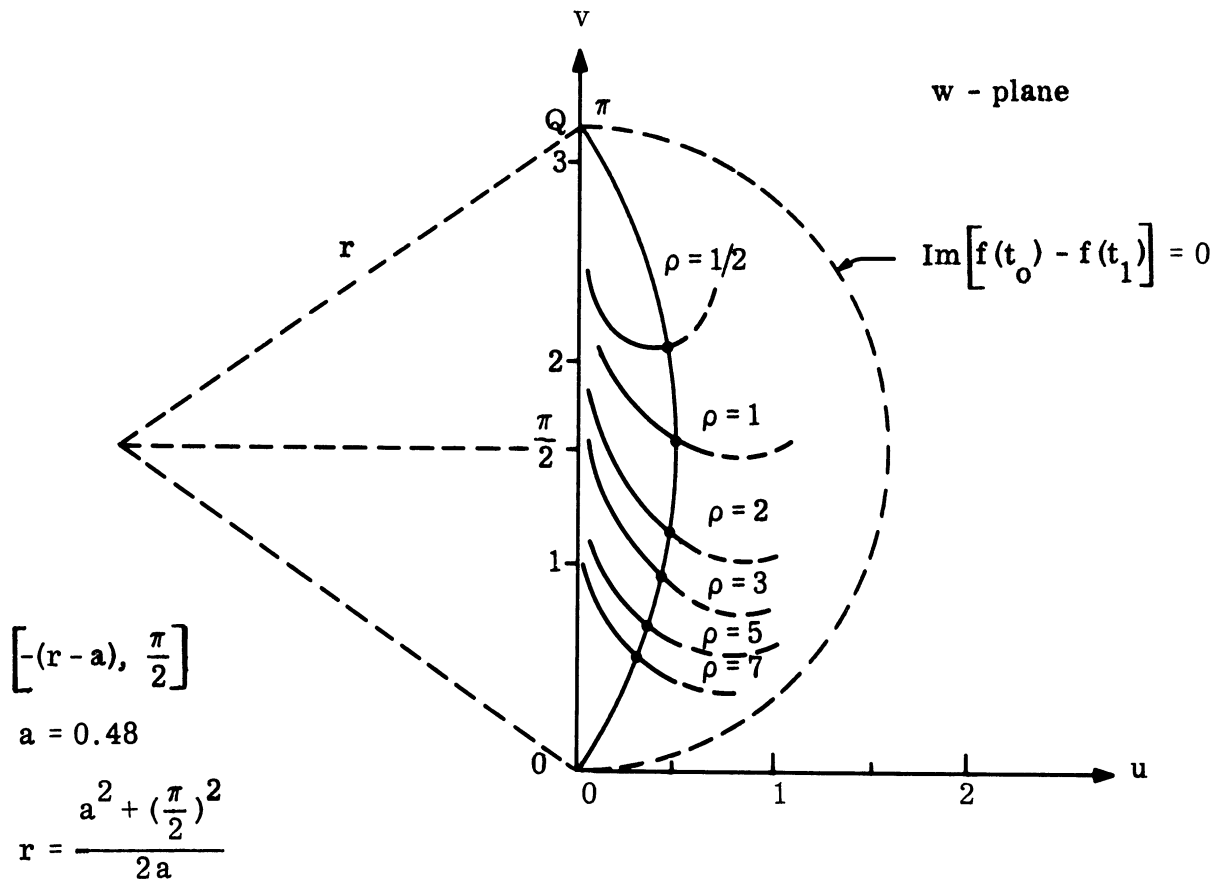


FIG. 3-5: GRAPHICAL SOLUTION FOR ZEROS OF $W_n(z)$ WHEN $z = \sqrt{-i} \rho$.

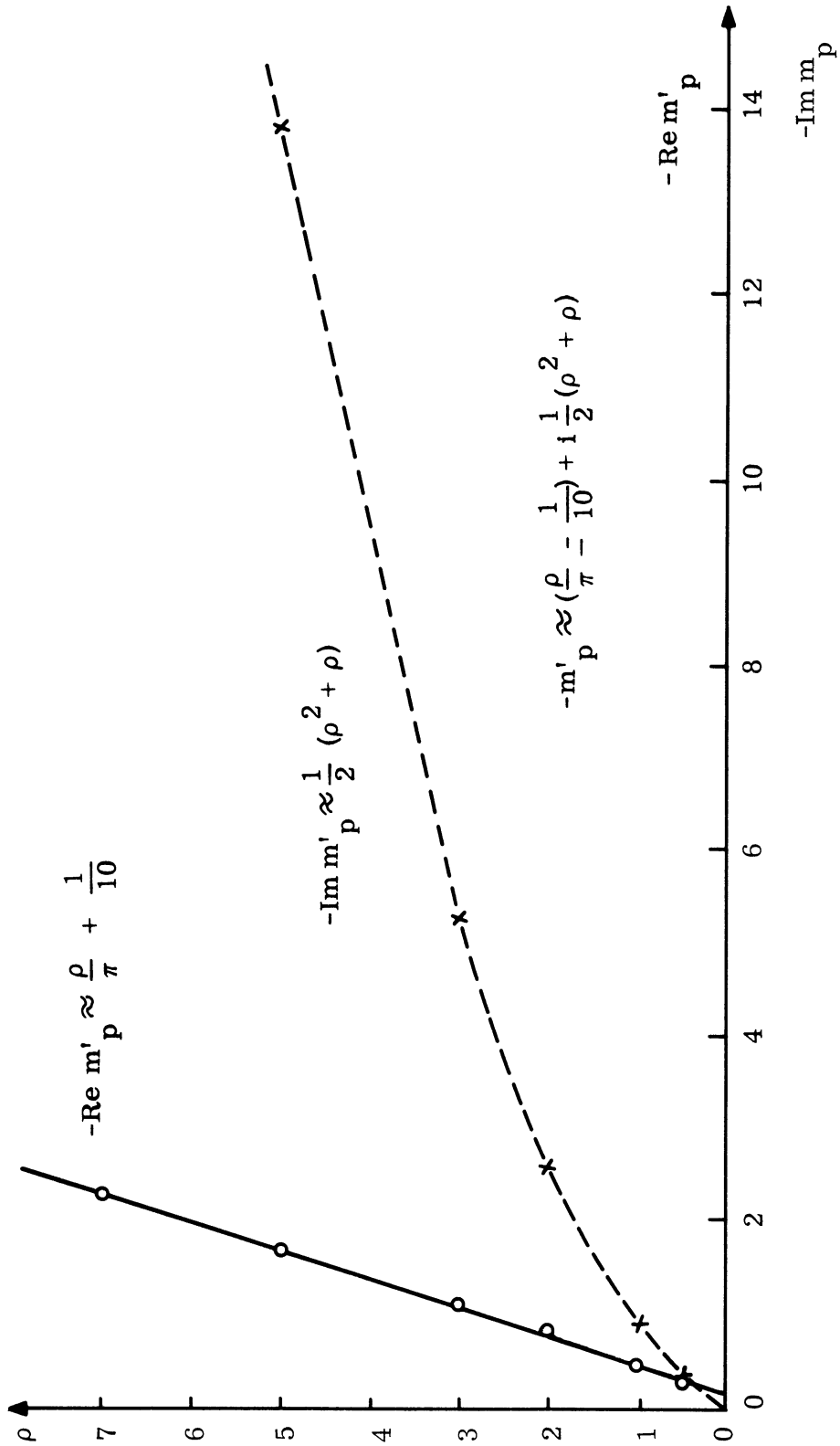


FIG. 3-6: LOCUS OF ZEROS OF $W_n(z)$ IN THE m -PLANE WHEN $z = \sqrt{-i} \rho$.

where

$$f(t) = -t^2 + 2z_0 t - (n+1) \ln t \quad . \quad (3.38)$$

Differentiating (3.37) we obtain the function $\frac{\partial}{\partial n} W_n(z_0)$ as

$$\frac{\partial}{\partial n} W_n(z_0) = -\frac{1}{2\pi i} \int_W (\ln t) e^{f(t)} dt \quad . \quad (3.39)$$

If we assume the path of integration W does not pass through the point $t = 0$, the function $\ln(t)$ may be considered as a slowly varying function in comparison with the integrand and put outside the integration sign at the saddle point. Therefore the saddle-point method may be applied to evaluate the asymptotic expression as the following

$$\begin{aligned} \frac{\partial}{\partial n} W_n(z_0) &\approx -(\ln t_0) \left[\text{contribution of } t_0 \text{ to } W_n(z) \right] - \\ &\quad - (\ln t_1) \left[\text{contribution of } t_1 \text{ to } W_n(z) \right] \\ &= -\left[(\ln t_0) A_0 - (\ln t_1) A_1 \right] \end{aligned} \quad (3.40)$$

where A_0 and A_1 are expressed by (3.13) and (3.14) respectively, and $z_0 = \sqrt{-2ikh} = \sqrt{-i}$. At the zero, $A_0 - A_1 = 0$, the asymptotic expression gives

$$\left. \frac{\partial}{\partial n} W_n(z_0) \right|_{n=n_s} = -\left[\ln(t_0/t_1) \right] A_0 \quad (3.41)$$

where n_s is the sth zero of $W_n(z_0)$ in the n -plane.

Next let us consider the definition

$${}'W_n(z_o) = -z_o W_n(z_o) + \frac{\partial}{\partial z_o} W_n(z_o) \quad (3.42)$$

By a similar consideration as before, we obtain the asymptotic expression for

$\frac{\partial}{\partial n} {}'W_n(z_o)$ as

$$\begin{aligned} \frac{\partial}{\partial n} {}'W_n(z_o) &\simeq -z_o \left[-(\ell n t_o) A_o + (\ell n t_1) A_1 \right] + \\ &\quad + 2 \left[-(\ell n t_o) t_o A_o + (\ell n t_1) t_1 A_1 \right] \\ &= -\sqrt{(z_o)^2 - 2m} \left[(\ell n t_o) A_o + (\ell n t_1) A_1 \right] \end{aligned} \quad (3.43)$$

At the zero, $A_o + A_1 = 0$, we obtain

$$\left. \frac{\partial}{\partial n} {}'W_n(z_o) \right|_{n=n'_s} = -\sqrt{(z_o)^2 - 2m'_p} \left[\ell n(t_o/t_1) \right] A_o \quad (3.44)$$

where n'_s is the s th zero of $'W_n(z_o)$ in the n -plane.

3.5 Creeping Waves

After zeros are obtained, the asymptotic expression of the function $U_n(z')$ in the region III was given by Rice (1954) as

$$U_n(z') = (1 - i^{4n}) A'_1 \quad (3.45)$$

where

$$A'_1 = \frac{\sqrt{t'_1} \exp f(t'_1)}{2\sqrt{\pi} (z^2 - 2m)^{1/4}}$$

$$\begin{aligned}
 z' &= \sqrt{ik}\xi \\
 f(t'_1) &= -t'_1{}^2 + 2z't'_1 - (n+1) \ln t'_1 \\
 t_1 &= \frac{1}{2} \left[\sqrt{ik}\xi - \sqrt{ik\xi^2 - 2m} \right] \\
 m &= n+1 \\
 &= m_p \text{ for Dirichlet's problem} \\
 &= m'_p \text{ for Neumann's problem} .
 \end{aligned} \tag{3.46}$$

Now we can evaluate (3.1) and (3.2). If we assume $\psi = \frac{\pi}{2}$ and consider the leading terms of the residue series, the surface currents in the shadow region become

$$\begin{aligned}
 J_D &= -2ki \sqrt{\frac{\pi}{kr}} \left[\frac{1}{\ln(t_o/t_1)} \right] \left[\frac{-i\rho^2 - 2m_p}{ik\xi^2 - 2m_p} \right]^{1/4} \\
 &\exp \left\{ \left(m_p - \frac{1}{2} \right) \ln \left[\frac{\sqrt{k\xi} + \sqrt{k\xi^2 + 2im_p}}{\sqrt{-2im_p}} \right] - i \frac{\sqrt{k}\xi}{2} \sqrt{k\xi^2 + 2im_p} + \right. \\
 &\left. + \left(m_p - \frac{1}{2} \right) \ln \left[\frac{\rho + \sqrt{\rho^2 - 2im_p}}{\sqrt{-2im_p}} \right] + i \frac{\rho}{2} \sqrt{\rho^2 - 2im_p} \right\} \tag{3.47}
 \end{aligned}$$

$$\begin{aligned}
 J_N = & - \frac{2 \sqrt{2\pi} i^{3/2}}{\ln(t_0/t_1) \left[(ik\xi^2 - 2m'_p)(-i\rho^2 - 2m'_p) \right]^{1/4}} \\
 & \exp \left\{ \left(m'_p - \frac{1}{2} \right) \ln \left[\frac{\sqrt{k\xi} + \sqrt{k\xi^2 + 2im'_p}}{\sqrt{-2im'_p}} \right] - i \frac{\sqrt{k}\xi}{2} \sqrt{k\xi^2 + 2im'_p} + \right. \\
 & \left. + \left(m'_p - \frac{1}{2} \right) \ln \left[\frac{\rho + \sqrt{\rho^2 - 2im'_p}}{\sqrt{-2im'_p}} \right] + i \frac{\rho}{2} \sqrt{\rho^2 - 2im'_p} \right\}. \quad (3.48)
 \end{aligned}$$

The asymptotic expressions obtained may be interpreted in terms of the "geometric theory of diffraction" (Keller, 1956). Let the length of the arc of the parabola between the points $\xi = 0$ and $\xi = \xi$ be

$$S = \int_0^\xi \sqrt{\xi^2 + 2h} d\xi = \frac{\xi}{2} \sqrt{\xi^2 + 2h} + h \ln \left[\frac{\xi + \sqrt{\xi^2 + 2h}}{2h} \right], \quad (3.49)$$

and the radius of curvature of the parabola at the point with coordinates $(\xi, 2h)$ is

$$R(\xi) = \frac{(\xi^2 + 2h)^{3/2}}{\sqrt{2h}}. \quad (3.50)$$

Finally let us express the integral over the arc of the parabola as

$$\begin{aligned}
 D &= \int_0^S \frac{ds}{[R(s)]^{2/3}} = (2h)^{1/3} \int_0^\xi \frac{d\xi}{(\xi^2 + 2h)^{1/3}} \\
 &= (2h)^{1/3} \ln \left[\frac{\xi + \sqrt{\xi^2 + 2h}}{\sqrt{2h}} \right]. \quad (3.51)
 \end{aligned}$$

Comparing these expressions with formulae (3.47) and (3.48), we obtain the asymptotic surface current in the forms

$$J_D/k \sim A(\rho) \frac{1}{\sqrt{k\rho}} [R(\xi)]^{-1/6} \exp \left\{ -ikS - \frac{k^{1/3}}{2} [(\rho+3.8) + i(\rho+1.4)] \frac{D}{\rho^{2/3}} \right\} \quad (3.52)$$

$$J_N \sim A'(\rho) [R(\xi)]^{-1/6} \exp \left\{ -ikS - \frac{k^{1/3}}{2} \left[\left(\frac{2\rho}{\pi} + 1.2 \right) + i\rho \right] \frac{D}{\rho^{2/3}} \right\} \quad (3.53)$$

where $A(\rho)$ and $A'(\rho)$ express amplitude functions which are a function of ρ only. Here $\rho = \sqrt{2kh}$.

Formulae (3.52) and (3.53) have the same expression as the results of Keller and Levy (1959). Therefore it is clear that the creeping wave theory may be extended into the region where the radius of curvature is comparable to the incident wavelength. The only place needing modification is the coefficient of D in the exponent of (3.52) and (3.53), where the coefficient is expressed as a function of the focal length $\rho = \sqrt{2kh}$. For large cylinders these coefficients are equal to $2.338 e^{i\pi/6}$ and $1.0188 e^{i\pi/6}$ for Dirichlet's and Neumann's problems respectively (Ivanov, 1960). In our case these coefficients are $[(\rho+3.8) + i(\rho+1.4)] / 2\rho^{2/3}$ and $[(\frac{2\rho}{\pi} + 1.2) + i\rho] / 2\rho^{2/3}$ in Dirichlet's and Neumann's problems respectively.

When the focal length of the parabolic cylinder is large compared to an incident wavelength, the asymptote of the function $W_n(z)$ may be expressed by Fock type formulae, i.e. the function can be expressed in terms of the Airy function (Rice, 1954; Ivanov, 1960). This is due to the fact that the asymptotic expressions given by the saddle-point method fail when m_p and m'_p are near $-ikh$, i.e. zeros of $W_n(z)$ are very close to $-(ikh+1)$. In this case two saddle points t_0 and t_1 coincide, and $f''(t_0)$ vanishes in Taylor expansion of the function $f(t)$. Therefore the unvanishing terms will start from the third derivative of the function $f(t)$, and the

asymptotic formulae may be expressed in terms of Airy integrals. In the case of the short focal length compared to the incident wavelength, the locations of zeros of the function $W_n(z)$ are not closed to $-(ikh + 1)$. Therefore the saddle-point method may be applied to evaluate the asymptotic expressions. This is what we have used to obtain the asymptotic formulae for surface currents in (3.47) and (3.48).

Let us define the surface currents as

$$\left| J_D/k \right| = A e^{-\alpha(\xi)} \tag{3.54}$$

$$\left| J_N \right| = A' e^{-\alpha'(\xi)} \tag{3.55}$$

where A and A' express the surface current density at the crest $\xi = 0$; $\alpha(\xi)$ and $\alpha'(\xi)$ are the attenuation factor as a function of the parabolic coordinate ξ . Then the surface current density at the crest is plotted approximately as a function of ρ in Fig. 3-7.

From Fig. 3-8 to Fig. 3-12, they show attenuation factors as a function of the parabolic coordinate ξ and of the arc length along the parabolic cylinder. Fig. 3-12 shows the constant attenuation contour on parabolic cylinders. The wavelength λ of the incident plane wave is plotted against parabolic cylinders for scaling. From these figures one can see that the attenuation factor for a large cylinder increases more rapidly than for a small one in the deep shadow region, i. e. the larger the cylinder the darker it is. In general it is much darker behind a parabolic cylinder than behind a half-plane. For the same cylinder, it is much darker for Dirichlet problem than for Neumann problem.

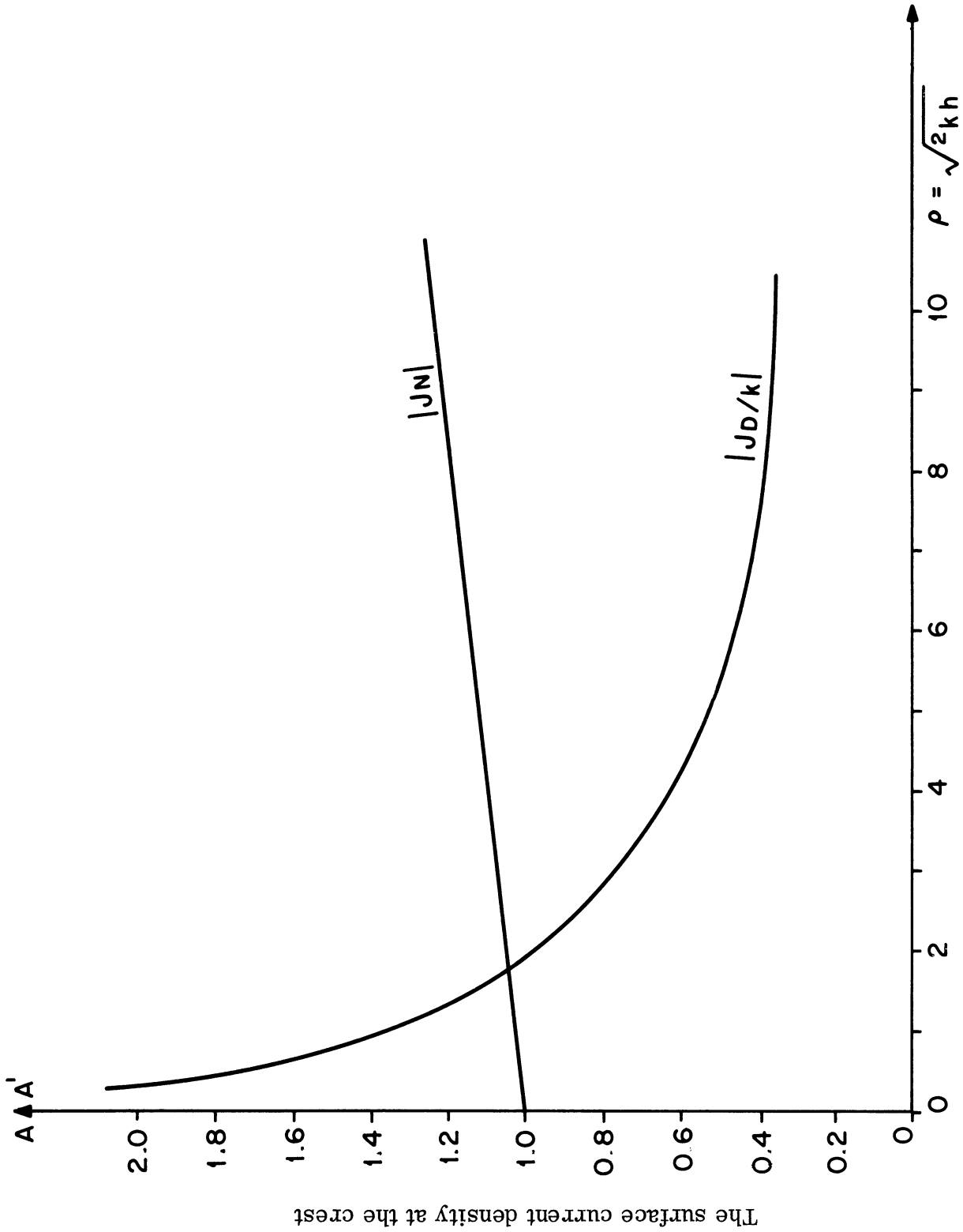


FIG. 3-7: THE SURFACE CURRENT DENSITY AT THE CREST, $\xi = 0$.

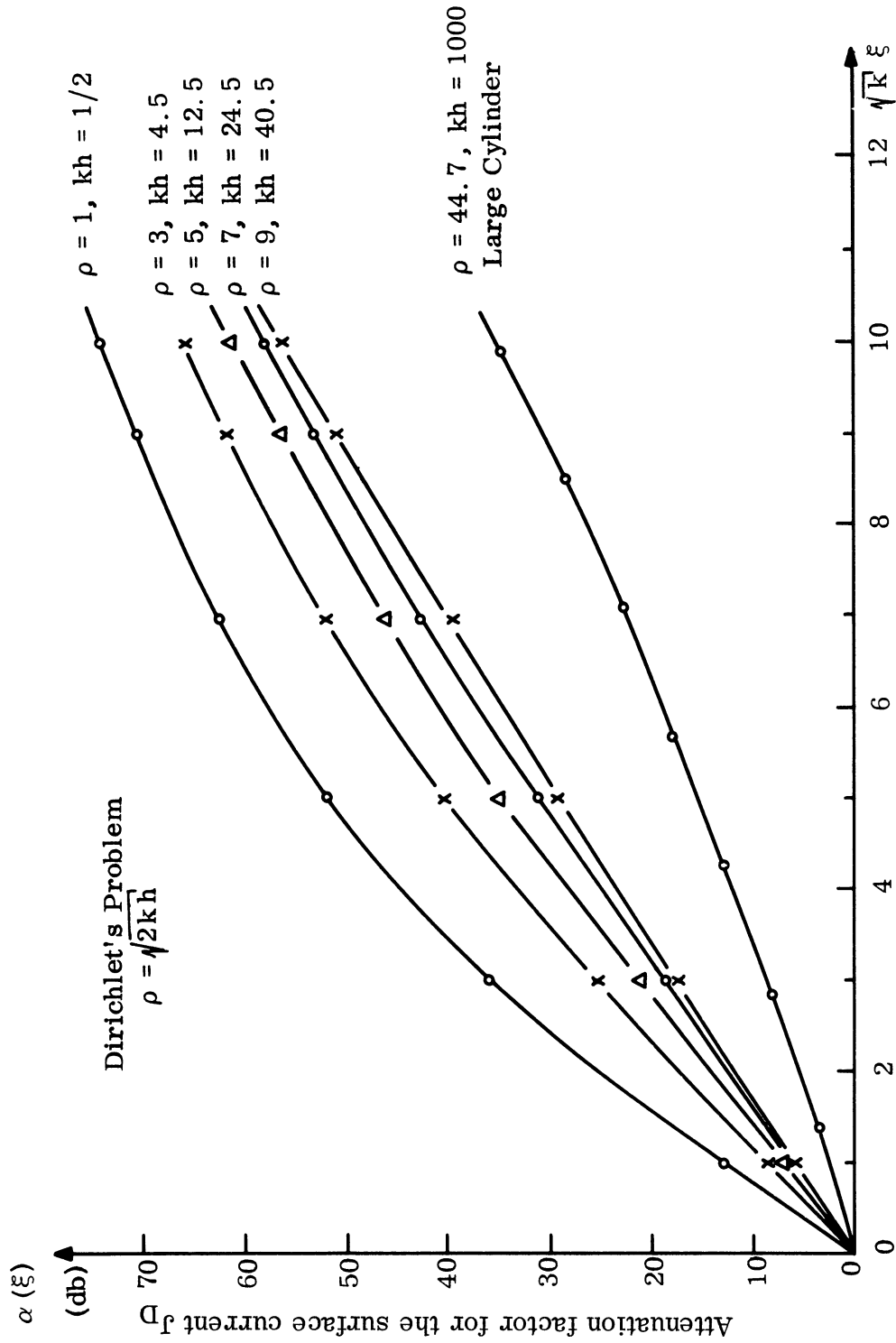


FIG. 3-8: $\alpha(\xi)$ VERSUS $\sqrt{k}\xi$.

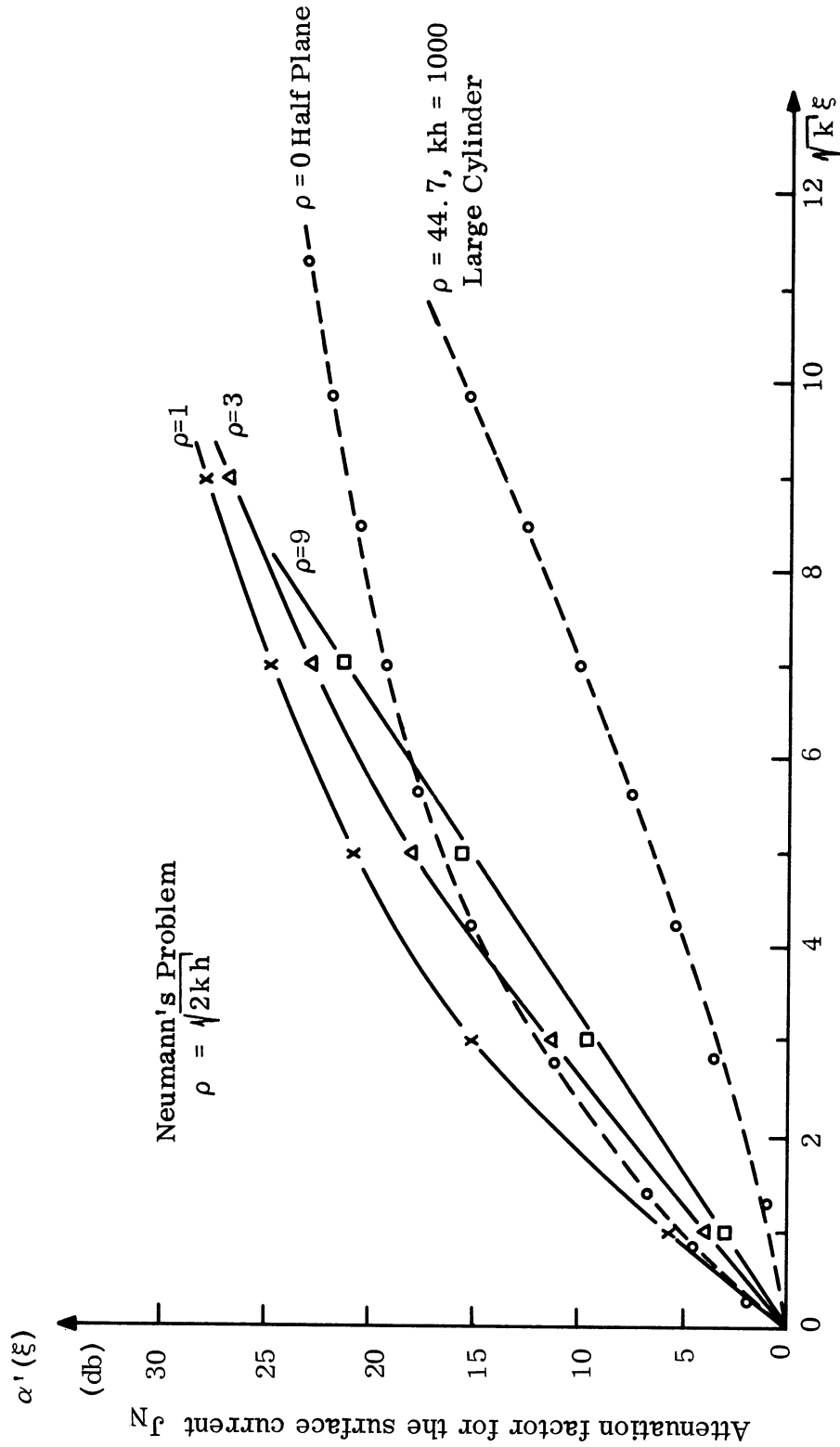


FIG. 3-9: $\alpha'(\xi)$ VERSUS $\sqrt{k}\xi$

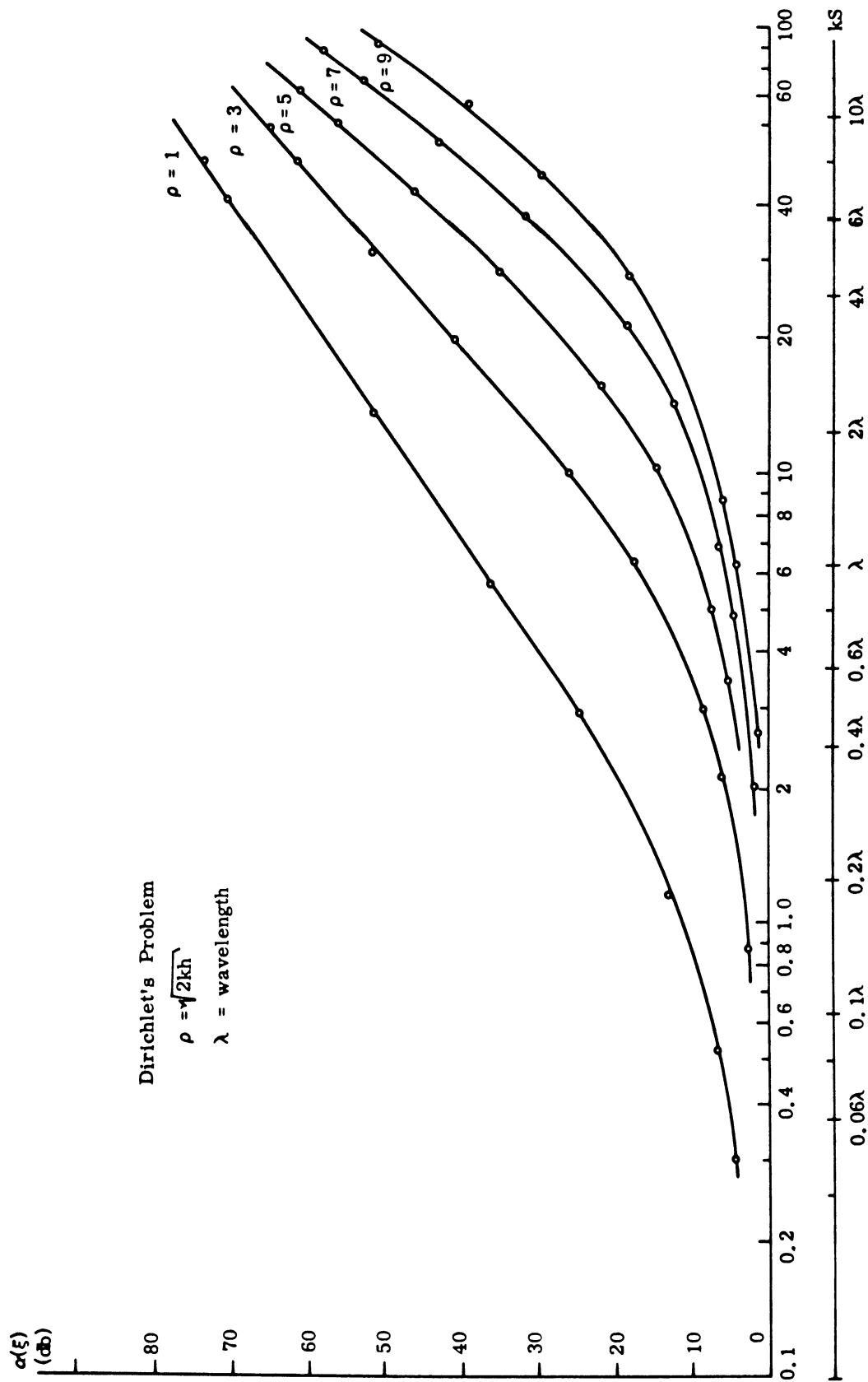


FIG. 3-10: ATTENUATION FACTOR FOR THE SURFACE CURRENT J_D VS THE ARC LENGTH ALONG THE PARABOLA.

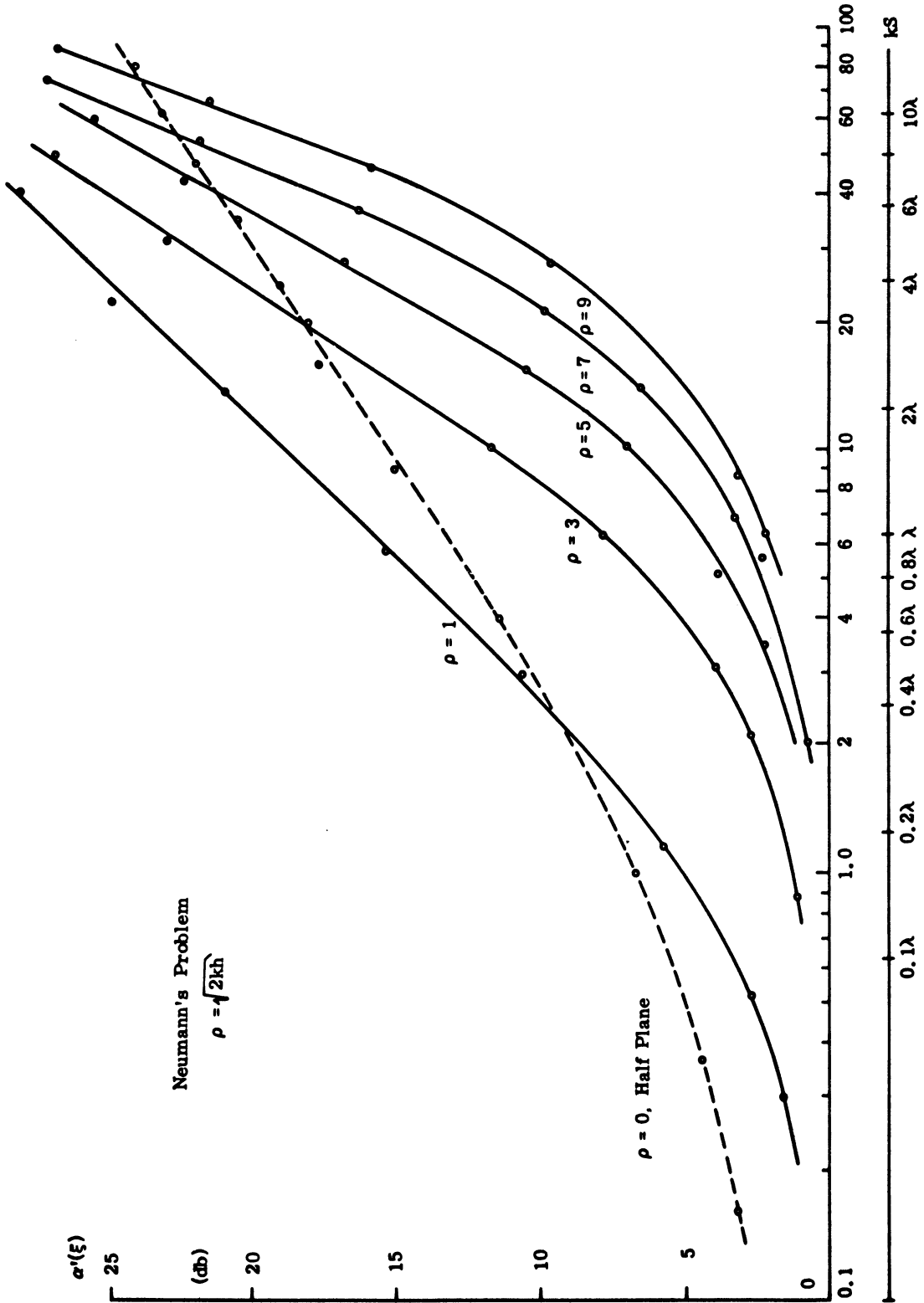


FIG. 3-11: ATTENUATION FACTOR FOR THE SURFACE CURRENT J_N VS THE ARC LENGTH ALONG THE PARABOLA.

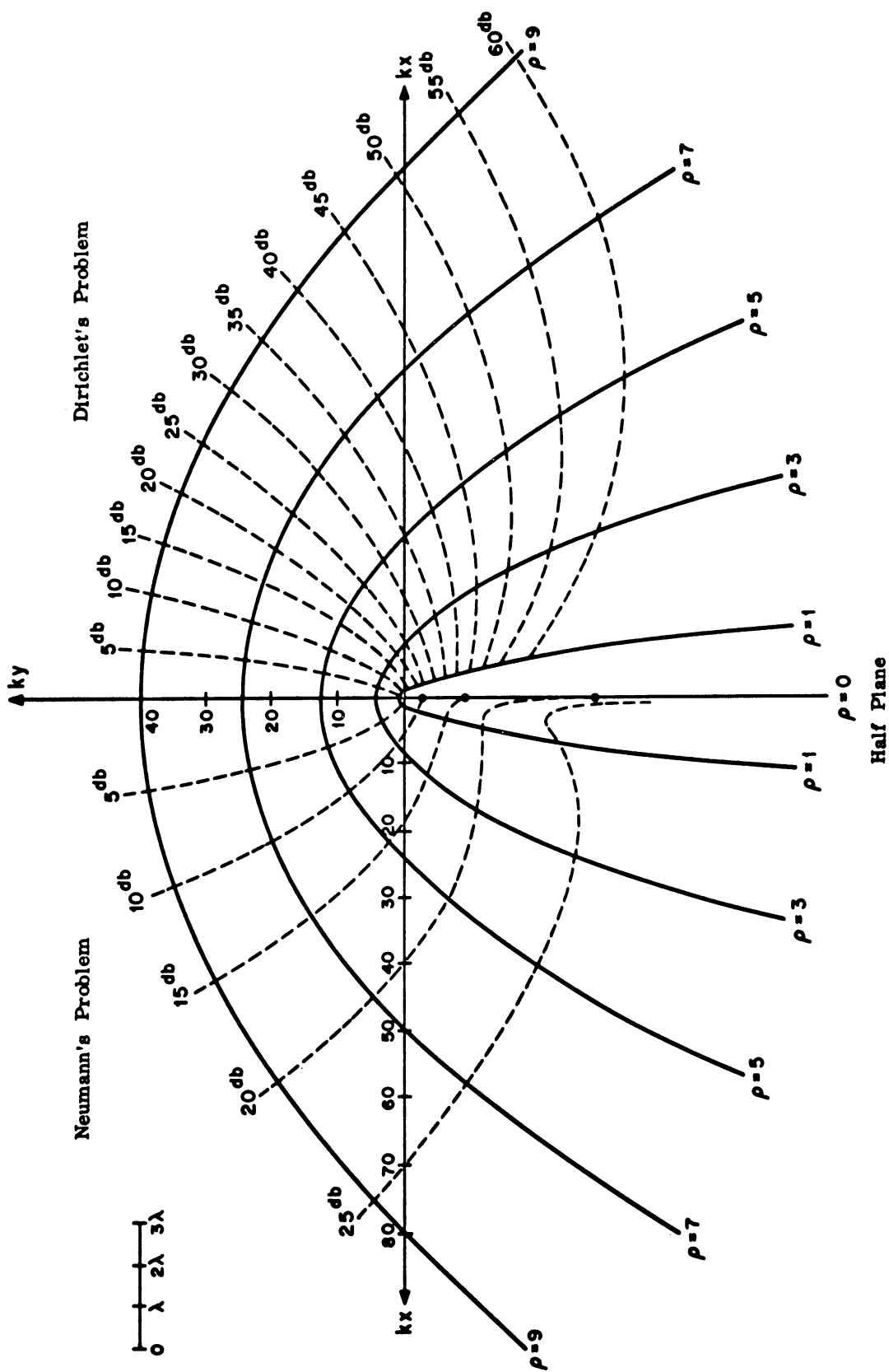


FIG. 3-12: ATTENUATION FACTORS ON PARABOLIC CYLINDERS.

IV

SURFACE CURRENTS IN THE ILLUMINATED REGION

4.1 Formulation

If we consider the region $x < 0$ where ξ is negative, we have the following relations

$$U_n(-z) = -i^{2n} V_n(z) - i^{-2n} W_n(z) \quad (4.1)$$

$$U_n(z) + V_n(z) + W_n(z) = 0 \quad (4.2)$$

Following Rice's (1954) derivation, the leading terms in the asymptotic expansion for $U_n(-z')$ along the contour C_2 is obtained as follows:

$$U_n(-z') = \left(i^{-2n} - i^{2n} \right) A'_0 + i^{-2n} A'_1 \quad (4.3)$$

$$A'_0 = \frac{\sqrt{t'_0} e^{f(t'_0)}}{2i\sqrt{\pi} (ik\xi^2 - 2m)^{1/4}}$$

$$A'_1 = \frac{\sqrt{t'_1} e^{f(t'_1)}}{2\sqrt{\pi} (ik\xi^2 - 2m)^{1/4}} \quad (4.5)$$

$$f(t') = zt' + \frac{m}{2} - m \ln t' \quad (4.6)$$

$$t'_0 = \frac{1}{2} \left[\sqrt{ik} \xi + \sqrt{ik\xi^2 - 2m} \right] \quad (4.7)$$

$$t'_1 = \frac{1}{2} \left[\sqrt{ik} \xi - \sqrt{ik\xi^2 - 2m} \right] \quad (4.8)$$

$$m = n + 1$$

$$z' = \sqrt{ik'} \xi, \quad \xi > 0.$$

In fact, the asymptotic expressions of the function $U_n(-z')$ in the various regions of the m -plane are listed in the following table when $z' = i^{1/2} \sqrt{k'} \xi$, $\sqrt{k'} \xi > 0$.

Region in m -plane $m = n + 1$	$U_n(-z')$
I _a	$(i^{-2n} - i^{2n}) A'_0 + i^{-2n} A'_1$
II	$-i^{2n} A'_0 + i^{-2n} A'_1$
I _b	$(i^{-2n} - i^{2n})(A'_0 + A'_1)$
III	$(i^{-2n} - i^{2n}) A'_0$

The contour C_2 passes through regions I_a and II in which $U_n(-z')$ has different asymptotic forms (Fig. 4-1). Because the stationary phase point z_0 is found within the region I_a, i.e.

$$-i\eta^2/2 < \alpha_0 < i\xi^2/2,$$

We may use the asymptotic form in I_a for $U_n(-z')$ along the entire contour C_2 .

When (4.3) is substituted into (2.7) and (2.8) we obtain

$$\begin{aligned}
 J_D = & \sqrt{\frac{k}{2\pi ri}} \frac{e^{-ikr}}{2} \sec \frac{\psi}{2} \left\{ -2i \int_{C_2} \left(i \tan \frac{\psi}{2} \right)^n \frac{A'_0}{W_n(z_0)} dn \right. \\
 & \left. + \int_{C_2} \left(\frac{\tan \frac{\psi}{2}}{i} \right)^n \frac{A'_1 dn}{\sin \pi n W_n(z_0)} \right\} \quad (4.9)
 \end{aligned}$$

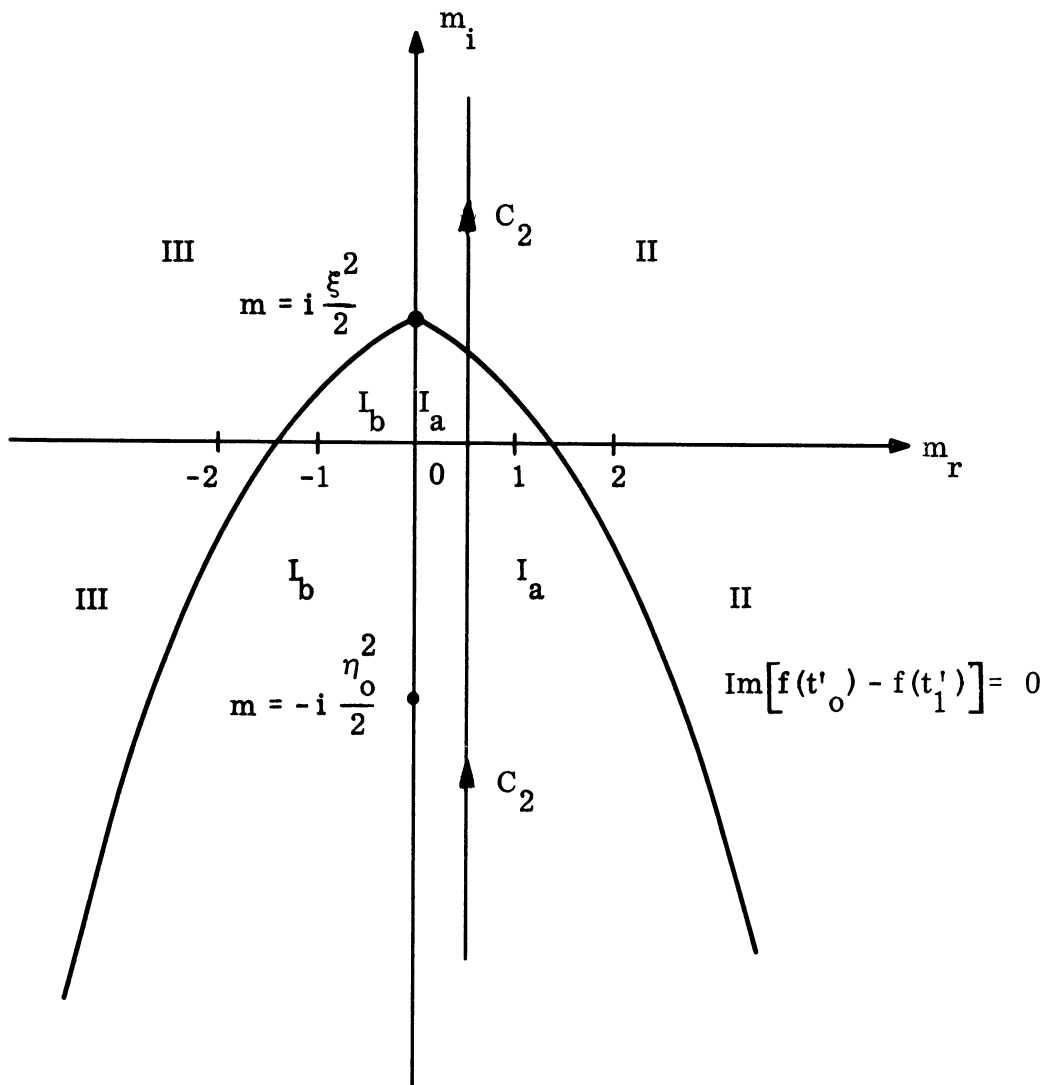


FIG. 4-1: REGION IN THE COMPLEX m -PLANE CORRESPONDING TO ASYMPTOTIC EXPRESSIONS WHEN $z = \sqrt{ik} \xi$.

$$\begin{aligned}
 J_N = & \frac{1}{\sqrt{\pi}} \frac{e^{-ikr}}{2} \sec \frac{\psi}{2} \left\{ -2i \int_{C_2} \left(i \tan \frac{\psi}{2} \right)^n \frac{A'_o}{W_n(z_o)} dn \right. \\
 & \left. + \int_{C_2} \left(\frac{\tan \frac{\psi}{2}}{i} \right)^n \frac{A'_1 dn}{\sin \pi n W_n(z_o)} \right\} \quad (4.10)
 \end{aligned}$$

In the following sections, we will see that the first term may be recognized as the geometrical optic term. The second term may be expressed by a residue series which represents creeping waves launched from the shadow boundary and traveling along the surface of the parabolic cylinder into the illuminated region. It may be called the reflected creeping waves (Fig. 1-1).

4.2 The Method of Geometrical Optics

The first term of (4.9) and (4.10) may be calculated by the stationary phase method when $k \rightarrow \infty$. The asymptotic forms of the functions $W_n(z_o)$ and $W'_n(z_o)$ along the contour C_2 were given by Rice (1954) as

$$W_n(z_o) = A_o \quad (4.11)$$

and

$$W'_n(z_o) = \sqrt{(z_o)^2 - 2m} A_o \quad (4.12)$$

Introducing the new variable of integration $\alpha = i \left(\frac{m}{k} \right)$, we obtain the first term of (4.9) and (4.10) as follows:

$$\begin{aligned}
 J_{D_o} = & \frac{-ik}{\sin \frac{\psi}{2}} \sqrt{\frac{k}{2\pi ri}} \int_{C_2} \left[\frac{\xi + \sqrt{\xi^2 + 2\alpha}}{\eta_o + \sqrt{\eta_o^2 - 2\alpha}} \right]^{1/2} \left[\frac{\eta_o^2 - 2\alpha}{\xi^2 + 2\alpha} \right]^{1/4} e^{-ik \Phi(\alpha)} d\alpha \quad (4.13)
 \end{aligned}$$

$$J_{N_0} = \frac{1}{\sin \frac{\psi}{2}} \sqrt{\frac{ik}{\pi}} \int_{C_2} \left[\frac{\xi + \sqrt{\xi^2 + 2\alpha}}{\eta_0 + \sqrt{\eta_0^2 - 2\alpha}} \right]^{1/2} \frac{e^{-ik \bar{\Phi}(\alpha)} d\alpha}{[(\xi^2 + 2\alpha)(\eta_0^2 - 2\alpha)]^{1/4}} \quad (4.14)$$

where

$$\begin{aligned} \bar{\Phi}(\alpha) = & \frac{\xi}{2} \sqrt{\xi^2 + 2\alpha} + \frac{\eta_0}{2} \sqrt{\eta_0^2 - 2\alpha} - \\ & - \alpha \ln \left[\omega \left(\frac{\eta_0 + \sqrt{\eta_0^2 - 2\alpha}}{\xi + \sqrt{\xi^2 + 2\alpha}} \right) \right] \end{aligned} \quad (4.15)$$

$$\omega = \tan \frac{\psi}{2}$$

The stationary point of the phase $\bar{\Phi}(\alpha)$ is obtained

$$\bar{\Phi}'(\alpha) = \ln \left[\omega \left(\frac{\eta_0 + \sqrt{\eta_0^2 - 2\alpha}}{\xi + \sqrt{\xi^2 + 2\alpha}} \right) \right] = 0$$

as

$$\omega \left(\eta_0 + \sqrt{\eta_0^2 - 2\alpha} \right) = \xi + \sqrt{\xi^2 + 2\alpha} . \quad (4.16)$$

The equation (4.16) has a real root if $\eta_0 \omega < \sqrt{\xi^2 + 2\alpha} + \xi$. On solving this inequality, we find

$$\xi > -\eta_0 \cot \psi .$$

The point $\xi = -\eta_0 \cot \psi$ is the boundary of the shadow and the points $\xi > -\eta_0 \cot \psi$ are located in the illuminated region. (g. 2-1). Thus the stationary point of the phase $\bar{\Phi}(\alpha)$ exists only if the point of observation is situated in the illuminated region. Solving (4.16), the stationary point is found as

$$\alpha_0 = \sin \psi \left(\frac{\eta_0^2 - \xi^2}{2} \sin \psi - \xi \eta_0 \cos \psi \right). \quad (4.17)$$

Substituting α_0 into the phase function $\Phi(\alpha)$ we have

$$\begin{aligned} \Phi(\alpha_0) &= \xi \eta_0 \sin \psi - \frac{\eta_0^2 - \xi^2}{2} \cos \psi \\ &= x \sin \psi - y \cos \psi \end{aligned} \quad (4.18)$$

and also

$$\sqrt{\xi^2 + 2\alpha_0} = \eta_0 \sin \psi - \xi \cos \psi$$

$$\sqrt{\eta_0^2 - 2\alpha_0} = \eta_0 \cos \psi + \xi \sin \psi$$

$$\Phi''(\alpha_0) = \frac{-1}{\sin \psi (\eta_0 \cos \psi + \xi \sin \psi) (\eta_0 \sin \psi - \xi \cos \psi)}$$

$$r = \frac{1}{2} (\eta_0^2 + \xi^2).$$

Now the asymptotic expressions of the surface current in the illuminated region are obtained as follows:

$$J_{D_0} = -2ik \frac{\eta_0 \cos \psi + \xi \sin \psi}{\sqrt{\xi^2 + \eta_0^2}} \left\{ \exp -ik (x \sin \psi - y \cos \psi) \right\} \quad (4.19)$$

$$J_{N_0} = 2 \exp \left\{ -ik (x \sin \psi - y \cos \psi) \right\}. \quad (4.20)$$

It has been shown that the quantity $(\eta_0 \cos \psi + \xi \sin \psi) / \sqrt{\xi^2 + \eta_0^2}$ in (4.19) is the cosine of the angle of incidence θ (Fig. 2-1), and the exponential factor is the incident plane wave U_0 (Ivanov, 1963). Thus

$$J_{D_0} = -2ik \cos \theta U_0 \quad (4.21)$$

$$J_{N_0} = 2 U_0 \quad (4.22)$$

i.e. the distribution of current in the illuminated region is described asymptotically by geometrical optics.

4.3 Reflected Creeping Waves

The second term of (4.9) and (4.10) may be calculated by the sum of the residues at poles given by $W_n(z_0) = 0$ and $'W_n(z_0) = 0$. Thus we obtain

$$J_{D_c} = \sqrt{\frac{ik\pi}{2r}} e^{-ikr \sec \frac{\psi}{2}} \sum_1^{\infty} \left[\frac{\left(\tan \frac{\psi}{2}/i\right)^n A'_1}{\sin \pi n \frac{\partial}{\partial n} W_n(z_0)} \right]_{n=n_s} \quad (4.23)$$

$$J_{N_c} = i \sqrt{\pi} e^{-ikr \sec \frac{\psi}{2}} \sum_0^{\infty} \left[\frac{\left(\tan \frac{\psi}{2}/i\right)^n A'_1}{\sin \pi n \frac{\partial}{\partial n} 'W_n(z_0)} \right]_{n=n'_s} \quad (4.24)$$

Comparing above expression with (3.1) and (3.2), one can see that the reflected creeping waves in the illuminated region are exactly the same with the transmitted creeping waves in the shadow region except for a constant factor

$$\frac{e^{-im\pi}}{(1 - e^{i2m\pi})}$$

Both are launched from the shadow boundary. One propagates into the illuminated region and the other into the shadow region. Let us define this constant factor as the ratio of reflection to transmission, then we have

$$C(m) = \frac{e^{-i m \pi}}{1 - e^{i 2 m \pi}} \quad (4.25)$$

where

$$\begin{aligned} m &= m_p \quad \text{for Dirichlet problem} \\ &= m'_p \quad \text{for Neumann problem} \end{aligned}$$

In general, $|C(m)|$ is negligibly small for $\rho > 1$ (Fig. 4-2). Therefore, reflected creeping waves may be neglected in the case of large parabolic cylinders.

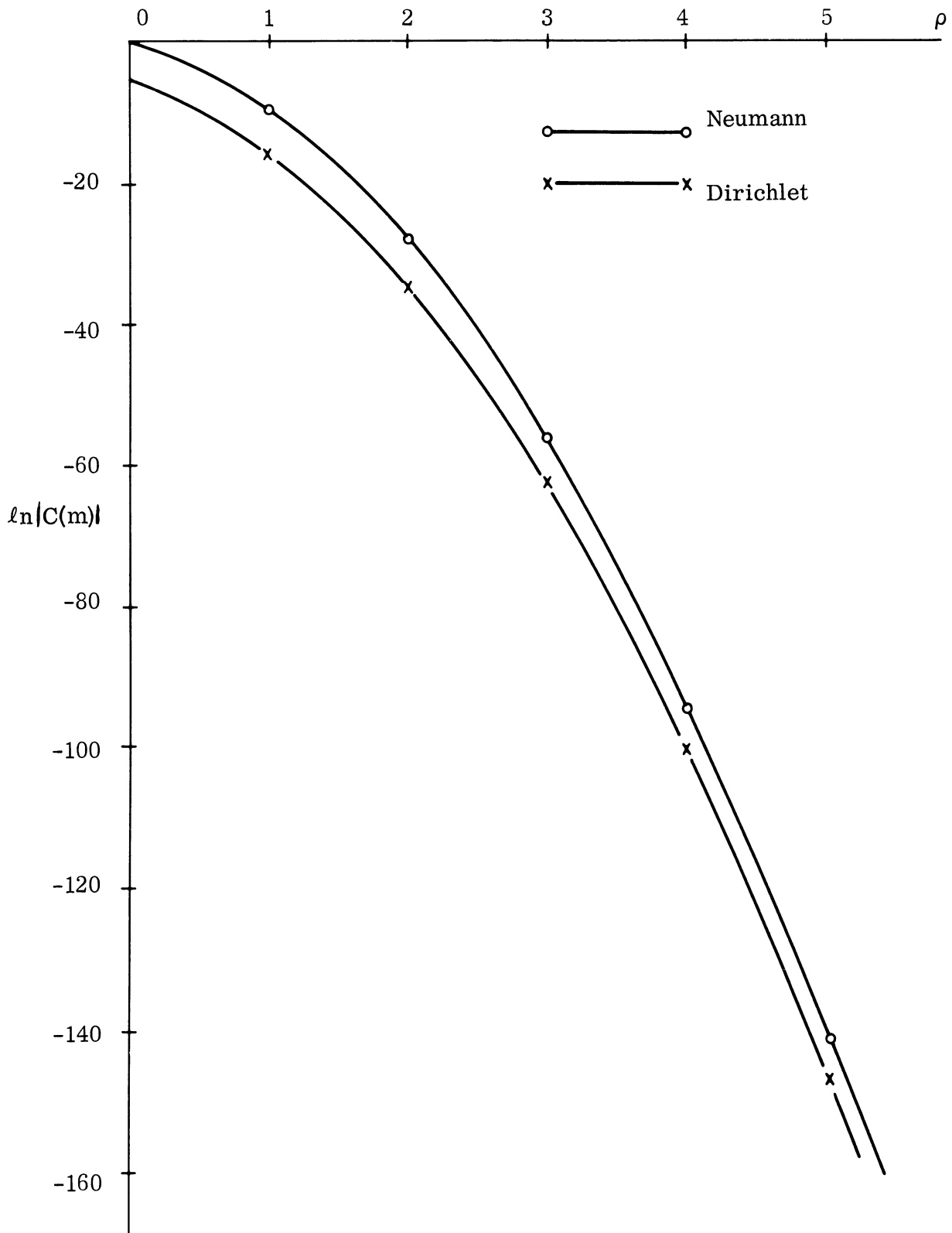


FIG. 4-2: $\ln |C(m)|$ VERSUS ρ .

V

THE SURFACE CURRENT IN THE REGION OF PENUMBRA

The function $U_n(z')$ in (2.7) and (2.8) may be expanded into a series about a point on the shadow boundary. If we expand $\exp(2z't)$ in the following integral

$$U_n(z') = \frac{1}{2\pi i} \int_u \exp \left\{ -t^2 + 2z't - (n+1) \ln t \right\} dt \quad (5.1)$$

and integrate termwise, then the function $U_n(z')$ becomes

$$U_n(z') = -\frac{\sin \pi n}{2\pi} \sum_{\ell=0}^{\infty} (-2z')^{\ell} \Gamma\left(\frac{\ell-n}{2}\right) / \ell ! \quad (5.2)$$

Therefore, we obtain the surface current in the following forms

$$J_D = +\frac{M_o}{2\pi} \sum_{\ell=0}^{\infty} \frac{(-2z')^{\ell}}{\ell !} \int_{C_2} \frac{(i\omega)^n \Gamma\left(\frac{\ell-n}{2}\right)}{W_n(z_o)} dn \quad (5.3)$$

$$J_N = +\frac{N_o}{2\pi} \sum_{\ell=0}^{\infty} \frac{(-2z')^{\ell}}{\ell !} \int_{C_2} \frac{(i\omega)^n \Gamma\left(\frac{\ell-n}{2}\right)}{W_n(z_o)} dn \quad (5.4)$$

where

$$M_o = \sqrt{\frac{k}{2\pi ri}} \frac{e^{-ikr}}{2} \sec \frac{\psi}{2}$$

$$N_o = \frac{1}{\sqrt{\pi}} \frac{e^{-ikr}}{2} \sec \frac{\psi}{2}$$

$$\omega = \tan \frac{\psi}{2} \quad .$$

Now (5.3) and (5.4) may be evaluated by the residue series. If only leading terms are considered, we obtain

$$\begin{aligned}
 J_D &= M_0 \frac{2\sqrt{\pi}(-i\rho^2 - 2m_p)^{1/4} (i\omega)^{n_s}}{\ln\left(\frac{t_0}{t_1}\right)\sqrt{t_0} e^{f(t_0)}} \sum_{\ell=0}^{\infty} \frac{(-2z')^{\ell}}{\ell!} \Gamma\left(\frac{\ell - n_s}{2}\right) \\
 &\approx -iM_0 \frac{2\pi (i\rho^2 - 2m_p)^{1/4} (\omega)^{n_s}}{\ln\left(\frac{t_0}{t_1}\right)\Gamma\left(-\frac{n_s}{2}\right)(2m_p)^{1/4}} \\
 &\quad \exp\left\{\left(m_p - \frac{1}{2}\right) \ln \frac{t_0}{\sqrt{2m_p}} - \sqrt{-i\rho} t_0\right\} \sum_{\ell=0}^{\infty} \frac{(-2z')^{\ell}}{\ell!} \Gamma\left(\frac{\ell - n_s}{2}\right) \quad (5.5)
 \end{aligned}$$

$$\begin{aligned}
 J_N &= N_0 \frac{2\sqrt{\pi}(i\omega)^{n'_s} e^{-f(t_0)}}{\ln\left(\frac{t_0}{t_1}\right)\sqrt{t_0}(-i\rho^2 - 2m'_p)^{1/4}} \sum_{\ell=0}^{\infty} \frac{(-2z')^{\ell}}{\ell!} \Gamma\left(\frac{\ell - n'_s}{2}\right) \\
 &\approx -iN_0 \frac{2\pi \sqrt{2} (\omega)^{n'_s}}{\ln\left(\frac{t_0}{t_1}\right) (2m'_p)^{1/4} \Gamma\left(-\frac{n'_s}{2}\right) (-i\rho^2 - 2m'_p)^{1/4}} \\
 &\quad \exp\left\{\left(m'_p - \frac{1}{2}\right) \ln \frac{t_0}{\sqrt{2m'_p}} - \sqrt{-i\rho} t_0\right\} \sum_{\ell=0}^{\infty} \frac{(-2z')^{\ell}}{\ell!} \Gamma\left(\frac{\ell - n'_s}{2}\right), \quad (5.6)
 \end{aligned}$$

where $z' = \sqrt{ik} \xi$, n_s and n'_s are zeros of $W_n(z_0)$ and $'W_n(z_0)$, respectively given by (3.24) and (3.36).

When $\omega = 1$, we have

$\xi > 0$ for the shadow region

$\xi < 0$ for the illuminated region .

Equations (5.5) and (5.6) converge absolutely for all finite values of ξ .

REFERENCES

- Epstein, P.S. (1914), Dissertation, Munich, see also the Encyklopädie der Math. Wiss. 5, Part 3 (1909-1926) Phys. , p. 511.
- Fock, V. (1946), "The Distribution of Currents Induced by a Plane Wave on the Surface of a Conductor," J. Phys. (USSR), 10 , pp. 130-136.
- Fock, V. (1946), "The Field of a Plane Wave Near the Surface of a Conducting Body," J. Phys. (USSR), 10, pp. 399-409.
- Ivanov, V.I. (1960), "Shortwave Asymptotic Diffraction Field in the Shadow of an Ideal Parabolic Cylinder," Radiotekhnika; elektronika, 5 , No. 3, pp. 393-402.
- Ivanov, V.I. (1963), "Diffraction of Short Plane Waves on a Parabolic Cylinder" Computational Mathematics and Mathematical Physics, No. 2, pp. 255-271.
- Keller J. B. (1956), "Diffraction by a Convex Cylinder," IRE Transactions on Antennas and Propagation, AP-4, pp. 312-321.
- Keller, J. B. and Levy, B.R. (1959), "Decay Exponents and Diffraction Coefficients for Surface Waves on Surfaces of Nonconstant Curvature," IRE Transactions on Antennas and Propagation, AP-7, pp. S52-S61.
- Rice, S.O. (1954), "Diffraction of Plane Radio Waves by a Parabolic Cylinder," Bell System Technical Journal , 33, pp. 417-504.

THE UNIVERSITY OF MICHIGAN

DISTRIBUTION LIST

Aerospace Corporation
ATTN: H.J. Katzman
Bldg. 537, Room 1007
P.O. Box 1308
San Bernardino, CA 92402
Copies 1-10 (incl.)

Air Force Cambridge Research Laboratories
ATTN: R. Mack CRDG
L.G. Hanscom Field
Bedford, MA 01730
Copies 11, 12

Advanced Research Projects Agency
ATTN: W. Van Zeeland
The Pentagon
Washington, D.C. 20301
Copies 13, 14

Air University Library
ATTN. AU
Maxwell AFB, AL 36112
Copy 15

Air Force Avionics Laboratory
ATTN: William F. Bahret - AVWE - 2
Wright-Patterson AFB, OH 45433
Copy 16

Space and Missile Systems Organization
ATTN: Capt. J. Wheatley, SMYSP
Norton AFB, CA 92409
Copies 17, 18

Space and Missile Systems Organization
ATTN: BSYLD
Norton, AFB, CA 92409
Copies 19, 20

Electronic Systems Division (AFSC)
ATTN: Lt. Nyman ESSXS
L.G. Hanscom Field
Bedford, MA 01730
Copy 21

THE UNIVERSITY OF MICHIGAN

Distribution List (Cont'd)

Institute for Defense Analyses
ATTN: Classified Library
400 Army-Navy Drive
Alexandria, VA 22202

Copy 22

MIT-Lincoln Laboratory Representative
P.O. Box 4188
Norton AFB, CA 92409

Copy 23

MIT-Lincoln Laboratory
BMRS Project Office
P.O. Box 73
Lexington, MA 02173

Copy 24

MIT-Lincoln Laboratory
ATTN: S. Borison
P.O. Box 73
Lexington, MA 02173

Copy 25

MIT-Lincoln Laboratory
ATTN: J. Rheinstein
P.O. Box 73
Lexington, MA 02173

Copy 26

MITRE Corporation
ATTN: P. Waterman
Bedford, MA 01730

Copy 27

North American Space
and Information Systems
ATTN: S. Wozniak
Tulsa, OK 73100

Copy 28

Special Projects Office,
Bureau of Weapons
ATTN: M. Blum
Washington, D.C. 20301

Copies 29, 30, 31

THE UNIVERSITY OF MICHIGAN

Distribution List (Cont'd)

Northrop-Norair Division
ATTN: F.K. Oshiro
3901 W. Broadway
Hawthorne, CA 90250

Copy 32

General Research Corporation
P. O. Box 3587
Santa Barbara, CA 93105

Copy 33

Ship Systems Analysis Branch
U. S. Naval Radiological Defense Lab.
ATTN: SABMIS
San Francisco, CA 94135

Copy 34

Space and Missile Systems Organization
ATTN: SMYS-1
Norton AFB, CA 92409

Copies 35, 36

Defense Documentation Center
Cameron Station
Alexandria, VA 22314

Copies 37 - 56 (incl.)

.....

DOCUMENT CONTROL DATA - R & D

(Security classification of title, body of abstract and indexing annotation must be entered when the overall report is classified)

1. ORIGINATING ACTIVITY (Corporate author) The University of Michigan Radiation Laboratory, Dept. of Electrical Engineering, 201 Catherine Street, Ann Arbor, Michigan 48108	2a. REPORT SECURITY CLASSIFICATION UNCLASSIFIED
	2b. GROUP

3. REPORT TITLE
SURFACE CURRENTS INDUCED BY A PLANE WAVE ON A PARABOLIC CYLINDER WITH A FOCAL LENGTH COMPARABLE TO THE INCIDENT WAVELENGTH.

4. DESCRIPTIVE NOTES (Type of report and inclusive dates)
Technical Report No. 4

5. AUTHOR(S) (First name, middle initial, last name)
Shun-Jen Houg , Raymond F. Goodrich

6. REPORT DATE November 1967	7a. TOTAL NO. OF PAGES 43	7b. NO. OF REFS 8
---------------------------------	------------------------------	----------------------

8a. CONTRACT OR GRANT NO. F 04694-67-C-0055 b. PROJECT NO. c. d.	9a. ORIGINATOR'S REPORT NUMBER(S) 8525-4-T
	9b. OTHER REPORT NO(S) (Any other numbers that may be assigned this report) SAMSO-TR-68-35

10. DISTRIBUTION STATEMENT
This document is subject to special export controls. Transmittal to foreign governments or nationals may be made only with prior approval of SAMSO (SMSD), Los Angeles AF Station, Los Angeles, California 90045.

11. SUPPLEMENTARY NOTES	12. SPONSORING MILITARY ACTIVITY Space and Missile Systems Organization (AFSC) Norton AFB, California 92409
-------------------------	---

13. ABSTRACT
Expressions are obtained for surface currents excited by a plane wave on the surface of a perfectly conducting parabolic cylinder whose focal length is comparable to the incident wavelength. In the shadow region, surface currents are expressed by the residue series which represents creeping waves propagating along the surface. In the illuminated region, surface currents may be represented by the summation of a geometrical optic term and a residue series which may be defined as the reflected creeping waves. In the penumbra region, surface currents may be obtained by the series expansion of the integral representation about a point on the shadow boundary.

14. KEY WORDS	LINK A		LINK B		LINK C	
	ROLE	WT	ROLE	WT	ROLE	WT
SURFACE CURRENTS CREEPING WAVES PARABOLIC CYLINDER INTEGRAL REPRESENTATION						

